1	Short Title:						
2	Physiological roles of phloridzin in apple						
3							
4							
5							
6	*Author for correspondence:						
7	Xiaoqing Gong and Fengwang Ma						
8	Tel.: +86-29-87082648						
9	E-mail addresses: gongxq0103@nwsuaf.edu.cn (X. Gong); fwm64@sina.com &						
10	fwm64@nwsuaf.edu.cn (F. Ma)						
11							
12							
13							
14							
15							
16							
17							
18							
19							
20							
21							
22							
23							
24							
25							
26							
27							
28							
29							
30							

31	MdUGT88F1-mediated phloridzin biosynthesis regulates apple development and Valsa
32	canker resistance
33	Kun Zhou ¹ , Lingyu Hu ¹ , Yangtiansu Li, Xiaofeng Chen, Zhijun Zhang, Bingbing Liu, Pengmin Li,
34	Xiaoqing Gong*, Fengwang Ma*
35	
36	State Key Laboratory of Crop Stress Biology for Arid Areas/Shaanxi Key Laboratory of Apple,
37	College of Horticulture, Northwest A&F University, Yangling, Shaanxi 712100, China
38	
39	
40	One-sentence summary:
41	MdUGT88F1-mediated phloridzin biosynthesis is critical for apple development and Valsa canker
42	resistance by regulating the interplay between cell wall deposition and accumulation of SA and
43	ROS.
44	
45	AUTHOR CONTRIBUTIONS
46	K.Z. and F.M. conceived the experiments; K.Z. and L.H. performed the experiments with
47	assistances from Y.L., F.C., Z.Z., and B. L.; X.G. and P.L. contributed to discussion; K.Z.
48	prepared the manuscript; and F.M. critically revised the manuscript.
49	
50	¹ These authors contributed equally to this work.
51	
52	*Address correspondence to gongxq0103@nwsuaf.edu.cn (X. Gong); fwm64@sina.com &
53	fwm64@nwsuaf.edu.cn (F. Ma)
54	
55	The author responsible for distribution of materials integral to the findings presented in this article
56	in accordance with the policy described in the Instructions for Authors (www.plantphysiol.org) is:
57	Fengwang Ma (fwm64@sina.com & fwm64@nwsuaf.edu.cn).
58	
59	
60	

ABSTRACT

61

62

63

64

65

66

67

68

69

70

71

72

73

74

75

76

77

In apple (Malus domestica), the polyphenol profile is dominated by phloridzin, but its physiological role remains largely elusive. Here, we used MdUGT88F1 (a key UDP-glucose: phloretin 2'-O-glucosyltransferase (P2'GT) gene) transgenic apple lines and Malus germplasm to gain more insight into the physiological role of phloridzin in apple. Decreasing phloridzin biosynthesis in apple lines by RNA silencing of MdUGT88F1 led to a series of severe phenotypic changes that included severe stunting, reduced internode length, spindly leaf shape, increased stem numbers, and weak adventitious roots. These changes were associated directly with reduced lignin levels and disorders in cell wall polysaccharides. Moreover, compact organization of tissues and thickened bark enhanced resistance to Valsa canker (caused by the fungus Valsa mali), which was associated with lignin- and cell wall polysaccharide-mediated increases of SA (salicylic acid) and ROS (reactive oxygen species). Phloridzin was also assumed to be utilized directly as a sugar alternative and a toxin accelerator by V. mali in apple. Therefore, after infection with V. mali, a higher level of phloridzin slightly compromised resistance to Valsa canker in MdUGT88F1 overexpressing apple lines. Taken together, our results shed light on the importance of MdUGT88F1-mediated biosynthesis of phloridzin in the interplay between plant development and pathogen resistance in apple trees.

78

Key words: Apple; Phloridzin; Plant development; Cell wall deposition; Valsa canker; Valsa mali

80

81

82

83

84

85

86

87

88

89

90

79

INTRODUCTION

Plants are exposed naturally to a large range of biotic and abiotic stresses and, therefore, they need to optimize their fitness by fine-tuning resource allocation for growth and defense (Huo et al., 2014). Plants frequently adopt a comprehensive defense against pathogen/pest threats at the expense of growth (Huo et al., 2014). A large number of structurally diverse molecules involved in plant-pathogen interactions and plant growth are produced by the phenylpropanoid pathway. The phenylpropanoid-derived polymer lignin is produced by oxidative polymerization of three monolignol precursors: *p*-coumaryl alcohol (H unit), coniferyl alcohol (G unit), and sinapyl alcohol (S unit); lignin cross-links plant secondary cell walls to provide mechanical strength and hydrophobicity to the vascular system necessary for the plant's ability to grow upward

(Nakashima et al., 2008; Vanholme et al., 2008; Van Acker et al., 2013) (Fig. 1). Frequently,
interference with lignin biosynthesis leads to growth defects. Intriguingly, lignin-reduced plants
exhibit an increase in both salicylic acid (SA) levels and SA-inducible pathogenesis-related (PR)
transcripts (Nakashima et al., 2008; Li et al., 2010; Lee et al., 2011; Gallego-Giraldo et al., 2011ab;
Van Acker et al., 2013). SA is a crucial phytohormone required for plant defense against pathogens
(Vlot et al., 2009). The intriguing relationship between SA and lignin levels is mainly attributed to
their biosynthetic overlap (Chen et al., 2009). There have been two major pathways proposed for
SA biosynthesis in plants (Fig. 1). The initial pathway is derived from the shikimic acid pathway
with isochorismate (Wildermuth et al., 2001). The secondary pathway through cinnamate involves
a benzoate 2-hydroxylase (León et al., 1995). Theoretically, any flux modifications to the lignin
pathway regulate the SA level. Alternatively, SA accumulation might result from the activation of
endogenous defense responses by elicitor-active polysaccharides released from improperly
lignified cell walls (Gallego-Giraldo et al., 2011ab).
Dihydrochalcones (DHCs) are phenylpropanoids that are very similar to chalcones
structurally, which are intermediates in flavonoid formation (Fig. 1). In apple (Malus domestica),
phloridzin (phloretin 2'-O-glucoside), which is the predominant DHC, comprises up to 90% of
soluble phenolic compounds in young shoots and leaves (Gosch et al., 2009). This makes apple
unique in the plant kingdom because phloridzin does not accumulate in such high amounts outside
Malus (Gosch et al., 2009). Variations in the DHC profile have been reported mostly within Malus,
but little is known about their physiological relevance (Zhou et al., 2017; 2018; Gutierrez et al.,
2018). Previous investigations reported that a Valsa canker-resistant apple, M. sieboldii,
accumulated less phloridzin than that of susceptible M. domestica. Moreover, the pathogen
degraded phloridzin directly for the production of toxins (i.e., phloroglucinol, protocatechuic acid,
p-hydroxybenzoic acid, 3-(p -hydroxyphenyl) propanoic acid, and p -hydroxyacetophenone) that
facilitated necrosis in apple bark (Koganezawa and Sakuma, 1982; Natsume et al., 1982; Wang et
al., 2014). Even so, there were no clear correlations between Valsa canker resistance and
phloridzin levels (Bessho et al., 1994).
Valsa canker, which is caused predominantly by the necrotrophic fungus Valsa mali, is one of
the most destructive diseases of apple in eastern Asia. Its successful infection only occurs in
wounded plants, although the conidia of the pathogen can germinate on both wounded and intact

barks. Infectious hyphae of <i>V. mali</i> can colonize, but not effectively degrade, xylem vessels (Yin et
al., 2015). After they infect wounded tissues, the pathogen hyphae develop inter- and
intracellularly and colonize all bark tissues, which results in severe tissue maceration and necrosis
(Yin et al., 2015). Then, the infection causes twigs, limbs, or entire trees to die, and the infection
can even cause entire orchards to fail (Ke et al., 2013). New lesions and infected trunks and shoots
mostly appear in spring, and the canker develops rapidly between spring and early summer, and
then slowly after that (Abe et al., 2007). Because of its perennial nature and the extensive
penetration of its pathogen into host phloem and xylem, Valsa canker cannot be controlled
effectively with agricultural chemicals (Yin et al., 2015). To date, microRNAs (Feng et al., 2017),
pathogenic effectors (Zhang et al., 2018), toxic compounds (Natsume et al., 1982; Wang et al.,
2014), and cell wall-degrading enzymes (Yin et al., 2015) have been implicated in the
pathogenicity of V. mali. Previous work has shed light on the management of apple Valsa canker.
Meanwhile, genetic engineering appears to be one of the most effective and practical methods to
control this infection. However, there is very limited knowledge on Valsa canker resistance in
apple.
As a side branch of the phenylpropanoid pathway, biosynthesis of phloridzin is mediated by
three successive steps: 1) NADPH-dependent formation of p-dihydrocoumaroyl-CoA from
p-coumaroyl-CoA by dehydrogenase (DH), 2) formation of phloretin from
p-dihydrocoumaroyl-CoA and three molecules of malonyl-CoA by the common chalcone synthase
(CHS), and 3) glycosylation of phloretin to phloridzin by UDP-glucose: phloretin
2'-O-glucosyltransferase (P2'GT) (Fig. 1) (Gosch et al., 2009; 2010). Previously, we identified a
key P2'GT, MdUGT88F1, which converted phloretin into phloridzin directly in apple (Zhou et al.,
2017). In this study, we analyzed comprehensively the physiological role of phloridzin using
MdUGT88F1 transgenic apple lines, which included overexpressing and silencing lines, and
Malus germplasm. Overall, our data clearly demonstrate that MdUGT88F1-mediated biosynthesis

RESULTS

Phloridzin biosynthesis is vital to apple growth

of phloridzin is critical for plant development and Valsa canker resistance by regulating the

interplay between cell wall deposition and accumulation of SA and ROS in apple trees.

We previously identified two P2'GTs, MdUGT88F1 and MdUGT88F4, that convert phloretin
into phloridzin in apple (Zhou et al., 2017). In this study, the expression of the key P2'GT gene
MdUGT88F1 was modified preferentially using a transgenic method. As a result, we obtained four
individual overexpressing (OE) lines and four individual RNA interference (RNAi). Two
pCambia2300-mediated OE lines, OE2-7 and OE3-4, and two pHellsgate2-mediated silencing
lines, Ri-3 and Ri-6, all of which displayed altered expression levels, were selected (Supplemental
Fig. S1). Slight phenotypic changes were only observed for Ri-3 and Ri-6 in tissue culture.
Moreover, many phenotypic changes, which included severe stunting, reduced internode length,
spindly leaf shape, more stems, and weak adventitious roots, were exhibited in RNAi apple lines
when transplanted from tissue culture to the greenhouse (Fig. 2A, 2B; Supplemental Table S1).
RT-qPCR analysis showed that these phenotypic changes in RNAi apple lines were associated
closely with reductions of MdUGT88F1 and MdUGT88F4 (Supplemental Fig. S1; Supplemental
Table S2). Because the sequences of MdUGT88F1 and MdUGT88F4 are highly similar (Zhou et
al., 2017), it was not possible to design primers to specifically knock-down either MdUGT88F1 or
MdUGT88F4 by RNAi. In contrast, OE2-7 and OE3-4 grew normally under both tissue-culture
and greenhouse conditions (Fig. 2A, 2B; Supplemental Table S1).
Analysis of the DHC profile revealed that there were no fluctuations observed in the OE
apple lines (Table 1). In contrast, in the RNAi apple lines, phloridzin levels were largely reduced,
and trilobatin appeared to accumulate significantly, which suggested decreased P2'GT activity
(Table 1). Moreover, under tissue-culture conditions, the application of phloridzin at 250 μM
significantly alleviated the retardation of leaf development and promoted branching in Ri-6, but
impeded the growth of GL-3 plantlets (Fig. 2C, 2D), which suggested an enhanced phloridzin
utilization efficiency in RNAi apple lines with reduced biosynthesis of phloridzin. Therefore,

A dwarf phenotype was closely associated with reduced lignin accumulation in RNAi apple lines

phloridzin biosynthesis is extremely vital to apple growth.

Differences in growth increased between GL-3 and RNAi apple lines that were grown in greenhouse conditions for 3 months. Intriguingly, there was a higher root-shoot ratio (dry weight and length) in Ri-3 (Fig. S2). Also, compared with those of GL-3, the thickened bark and reduced

xylem in the stems of Ri-3 suggested a reduction of lignin (Fig. 3A, 3B). Analysis of lignin verified that the cell wall residue (CWR) and acetyl bromide (AcBr) total lignin were reduced by 18.5% and 18.7%, respectively, in the stems of Ri-3, but not in roots (Fig. 3C, 3D), which accounted for the higher root-shoot ratio.

181

182

183

184

185

186

187

188

189

190

191

192

193

194

195

196

197

198

199

200

201

202

203

204

205

206

207

208

209

210

Cellular organization of transgenic apple lines and GL-3 was examined by toluidine blue O staining (Fig. 4A-D). Cross sections of leaves from Ri-3 revealed more compacted epidermal cells, a thicker palisade, and disorderly vascular bundles in the main veins compared with GL-3 (Fig. 4A). The spindly shape of RNAi apple leaves was associated mainly with a smaller angle between main and lateral veins, which reflected a disordered arrangement of the vascular bundle (Fig. 4E, 4F). Cross sections of the stems of Ri-3 showed that reduced xylem coexisted with expanded phloem, parenchyma, and pith. The decreased xylem also resulted in vessels with smaller sizes and lower densities (Fig. 4B). In addition, there were compacted epidermal cells and parenchyma cells with different shapes in Ri-3 stems (Fig. 4B, 4C). It is quite possible that these cellular changes made RNAi apple lines more resistant to V. mali (e.g., more compact cells may limit spread of the pathogen). In contrast, there appeared to be no obvious leaf and stem changes in the OE apple lines (Fig. 4A, 4B). Vascular bundles of the transgenic and non-transgenic apple roots were basically similar in morphology (Fig. 4D). β-glucuronidase (GUS) staining showed that there was obvious GUS activity in the stem vascular bundles of lines expressing ProMdUGT88F1:GUS, but not in an Arabidopsis thaliana line expressing ProMdUGT88F4:GUS (Supplemental Fig. S3), which supported the hypothesis that MdUGT88F1-mediated phloridzin biosynthesis plays an important role in the development of stem vascular bundles. Indeed, Gaucher et al. (2013a) also found that dihydrochalcones localized around the vascular system in apple.

Results from Wiesner and Mäule staining further confirmed that there were less lignin or fewer cells that contained lignin (i.e., a smaller xylem region in RNAi apple stems) (Fig. 4G, 4H). Metabolic analysis revealed that *p*-coumaric acid and hydroxycinnamoyl derivatives were greatly reduced in RNAi apple leaves (Supplemental Table S3). Among these decreased derivatives, *p*-coumaryl alcohol and sinapaldehyde participate directly in the biosynthesis of H- and S-lignin, respectively. However, there were no differences among the precursors of G-lignin, which include coniferaldehyde and coniferyl alcohol. Taken together, the dwarf phenotype of the RNAi apple

lines was closely associated with reduced lignin accumulation.

Abnormal composition of cell wall polysaccharides mediated by *myo*-inositol metabolism contributed partly to growth reduction in RNAi apple lines

Theoretically, UDP-glucose fluctuations resulted in changes in sugar metabolism in phloridzin biosynthesis-decreased RNAi apple lines. Metabolic analysis showed that the levels of glucose and *myo*-inositol decreased significantly in RNAi apple leaves, where values were 46-58% and 45-61% of those measured in GL-3, respectively (Supplemental Table S3). Such reductions were further verified by GC-MS analysis. For glucose, there appeared to be a slight increment in OE apple stems. However, there were significant reductions found in both leaves and stems of RNAi apple lines (Fig. 5A). There were no differences among *myo*-inositol levels found in leaves or stems of OE apple lines. In contrast, *myo*-inositol levels decreased in leaves and, in particular, stems of RNAi apple lines (Fig. 5B).

To test if myo-inositol reduction partly accounted for the stunted growth observed in RNAi apple lines, we conducted a myo-inositol depletion assay. Under MS control conditions, leaf shapes of OE2-7, Ri-6, and GL-3 were basically the same. However, under myo-inositol depleted conditions, stunted leaf growth occurred only in Ri-6, which indicated that the dwarf phenotype may be related to myo-inositol reduction in RNAi apple lines (Fig. 5C, 5D). RNA-seq analysis also revealed that two Galactinol synthase (GolS) genes were highly up-regulated in RNAi apple leaves (Supplemental Table S2). In Arabidopsis, GolS enzyme directly converted myo-inositol into galactinol for the biosynthesis of raffinose-family oligosaccharides, and it affected the composition of cell wall polysaccharides indirectly (Valluru and den Ende, 2011). Because there were glucose and myo-inositol reductions in the RNAi apple lines, we analyzed cell wall polysaccharides in the stems of transgenic apple lines and GL-3. Levels of cellulose and total pectic materials were essentially the same in transgenic and non-transgenic apple plants (Supplemental Fig. S4), but different pectic compositions were found in both Ri-3 and Ri-6. The cold water-soluble (WS) pectins increased at the expense of the EDTA-soluble pectic materials (Fig. 5E). Thus, the decreased biosynthesis of phloridzin probably disturbed the composition of cell wall polysaccharides through myo-inositol metabolism in RNAi apple lines.

Decreased biosynthesis of phloridzin significantly enhanced resistance to Valsa mali in RNAi

apple lines

Previous studies suggested that phloridzin might increase susceptibility to *Valsa* canker in apple (Koganezawa and Sakuma, 1982; Bessho et al., 1994). Accordingly, transgenic and non-transgenic apple leaves (Fig. 6A, 6C) and stems (Fig. 6B, 6D) were inoculated with *V. mali*. Three days after inoculation, lesions were observably smaller in RNAi apple lines and slightly larger in OE apple lines compared with GL-3. Also, RT-qPCR showed that OE apple lines and GL-3 responded to infection by down-regulating *MdUGT88F1* and *MdUGT88F4* (Fig. 6E, 6F). However, it is very difficult to assess the transcriptomic effects of *V. mali* on *MdUGT88F1* when RNAi apple lines were also being actively silenced for this gene (Fig. 6E, 6F). Meanwhile, in leaves of GL-3, phloridzin was reduced significantly by *V. mali*. But a relatively lower reduction led to a higher phloridzin accumulation in OE apple leaves after *V. mali* infection. Yet, there were very small changes following infection in RNAi apple leaves (Fig. 6G), although there still appeared to be a reduction in trilobatin (Fig. 6H). Phloretin was reduced in the leaves of RNAi apple lines, but was unchanged in both GL-3 and OE apple leaves (Fig. 6I). Thus, MdUGT88F1-mediated phloridzin biosynthesis appeared to have a negative effect on *Valsa* canker resistance in apple.

Phloridzin was utilized directly as a sugar alternative and a toxin accelerator by Valsa mali

To elucidate the mechanism of phloridzin in resistance to *Valsa* canker, the correlation between bark phloridzin levels and *Valsa* canker resistance in *Malus* was investigated based on our previous investigation (Zhou et al., 2017) (Supplemental Table S4). Although there were no significant correlations found, we observed a connection between *Valsa* canker susceptibility and an increase in DHC content (Supplemental Fig. S5A). Next, two *Malus* accessions that displayed contrasting susceptibilities to *V. mali* (i.e., susceptible and higher DHC-apple ZD1 (*M. hupehensis* Rehd.) compared with a lower-DHC and resistant apple ZH16 (*M. toringo*)), were selected for further analysis (Supplemental Fig. S5B, S5C). In ZD1, a decrease in DHC-glucosides and an increase in aglycone phloretin indicated that deglycosylation of DHC-glucosides occurred in response to *V. mali* invasion. In ZH16, there was a similar trend for DHCs upon infection with *V. mali*, although there were no significant differences (Supplemental Fig. S5D). Furthermore,

β-glucosidase activity in the infected bark increased gradually in both ZD1 and ZH16 (Supplemental Fig. S5E). Both phloridzin and phloretin were characterized by a weakly antimicrobial property towards *V. mali* (Supplemental Fig. S6). However, phloridzin (0.5 mM) remained favorable for *V. mali* growth. We observed accelerated deglycosylation of phloridzin followed by rapid degradation of phloretin once glucose was depleted in lines inoculated with *V. mali* (Fig. 7A-C; Supplemental Fig. S6C, S6D). Thus, we concluded that *V. mali* hydrolyzed phloridzin and consumed glucose by releasing β-glucosidase in barren apple bark. Additionally, 48 hours after incubation of *V. mali*, only the residual liquid from phloridzin-added normal potato dextrose broth (PDB) caused obvious necrosis in apple leaves (Fig. 7D). Thus, it appeared that phloridzin also accelerated tissue necrosis by facilitating production of toxins by *V. mali* (Fig. 7).

Gene expression analysis showed that *UGT88F1* and *UGT88F4* were down-regulated in both

ZD1 and ZH16 apple bark after infection by *V. mali*, although both *phenylalanine ammonia lyase* (*PAL*) and *CHS* were induced (Supplemental Fig. S7). Generally, plants employ multiple mechanisms to protect themselves from pathogen infection. The down-regulated expression of *UGT88F1* in both resistant and susceptible apples reflected a common involvement of phloridzin in *Valsa* canker resistance. Moreover, the negative involvement of phloridzin was also verified in transgenic apple lines. Thus, the MdUGT88F1-mediated phloridzin biosynthesis would be one of the factors that determined resistance to *Valsa* canker in apple trees. That is, phloridzin was utilized directly as a sugar alternative and a toxin accelerator for *V. mali* in apple.

Levels of SA and reactive oxygen species (ROS) are implicated in *Valsa* canker resistance in apple

RNA-seq analysis revealed that a large number of genes involved in plant-pathogen interactions (e.g., *PR* genes and SA biosynthesis regulatory genes) were largely induced in RNAi apple leaves (Supplemental Table S2). RT-qPCR demonstrated that the expressions of *MdPR1*, *MdPR2*, *MdPR4*, *MdPR5*, and *MdPR8* were largely up-regulated in RNAi apple leaves, but remained unchanged in OE apple leaves (Supplemental Fig. S8A). Phytohormone analysis verified that both free SA and total SA were largely accumulated in RNAi apple leaves, but only total SA was reduced slightly in OE3-4 leaves (Fig. 8A, 8B). Moreover, these *PRs* were differentially up-regulated in leaves from transgenic apple lines and GL-3 in response to *V. mali*

infection (Fig. 8D). Compared with GL-3, higher expression was still shown in RNAi apple lines, but in OE apple lines, lower levels of *MdPR1* and *MdPR2* and similar accumulation of *MdPR4*, *MdPR5*, and *MdPR8* were found (Fig. 8D). The up-regulated *PR* genes (Supplemental Fig. S8B) and increased SA levels (Fig. 8C) in both ZD1 and ZH16 upon infection with *V. mali* suggested a positive role of SA in *Valsa* canker resistance in apple.

DHCs are considered to be excellent antioxidant compounds (Dugé de Bernonville et al., 2010; Xiao et al., 2017). In particular, the large reductions in phloridzin (Table 1) and hydroxycinnamoyl derivatives (Supplemental Table S3) certainly would interfere with the redox state in RNAi apple lines. Staining with nitro blue tetrazolium (NBT) and diaminobenzidine (DAB) revealed a strong increase in hydrogen peroxide (H₂O₂) and superoxide ion (O₂) accumulation in leaves of RNAi lines when compared with those of GL-3, although there were no significant differences in leaves of OE lines (Fig. 9A). In addition, metabolic analysis showed that levels of oxidized and reduced glutathione (i.e., GSSH and GSH) decreased in RNAi apple leaves to approximately 28% and 25% of those measured in GL-3, respectively. Also, there was a slight reduction in L-ascorbate (AsA) (Supplemental Table S3). Such reductions largely accounted for the high ROS accumulation in RNAi apple lines. Moreover, H₂O₂ was differentially induced in transgenic and non-transgenic apple leaves after infection by V. mali. (Fig. 9B). Although there were no differences between GL-3 and OE lines under controlled conditions, lower induction levels resulted in lower H₂O₂ accumulation in both OE lines upon infection with V. mali. In contrast, rare inductions resulted in comparable H₂O₂ levels in GL-3 and RNAi apple leaves (Fig. 9B), which suggested that a higher pre-challenge level of H₂O₂ was important (Fig. 9C, 9D). In addition, in susceptible ZD1, H₂O₂ decreased gradually after infection by V. mali (Fig. 9C). However, in resistant ZH16, H₂O₂ was induced rapidly and remained at a relatively higher level (Fig. 9D). This indicated that ROS levels played a key role in Valsa canker resistance in apple. In summary, after pathogen infection, decreased phloridzin biosynthesis increased the levels of SA and ROS, which enhanced Valsa canker resistance in apple.

327

328

329

330

301

302

303

304

305

306

307

308

309

310

311

312

313

314

315

316

317

318

319

320

321

322

323

324

325

326

DISCUSSION

Phloridzin appears to play important physiological roles in plant development and pathogen defense in apple (Zhang et al., 2007; Dare et al., 2013; Hutabarat et al., 2016). In the present study,

we used *MdUGT88F1*, the key *P2'GT* gene, transgenic apple lines and wild *Malus* accessions to gain new insight into the functions of phloridzin in apple. Overall, our results provided insight into the importance of MdUGT88F1-mediated phloridzin biosynthesis in the interplay between plant development and pathogen resistance in apple trees.

We observed a severe reduction in growth in the MdUGT88F1-RNAi apple lines with decreased phloridzin biosynthesis. Other researchers also reported a very similar phenotype in *UGT88F1* silencing lines (Dare et al., 2017). Results from Dare et al. (2017) and this study revealed the presence of trilobatin in the *MdUGT88F1* silencing lines, which indicated that decreased P2'GT activity led to a higher conversion of phloretin to trilobatin by UDP-glucose: phloretin 4'-*O*-glucosyltransferase (P4'GT). Interestingly, a *P4'GT* gene, *MdPh-4'-OGT*, was previously identified and found to be expressed in 'Golden Delicious' apple, which does not accumulate trilobatin (Yahyaa et al., 2016). Independent silencing of *CHS* and *UGT88F1* also resulted in similar phenotypes in apple (Dare and Hellens, 2013; Dare et al., 2013; 2017). However, such phenotypic changes were not found in CHS null mutants from *Arabidopsis*, a species that lacks phloridzin accumulation (Shirley et al. 1995; Li et al., 2010). Thus, these results collectively indicated that decreased biosynthesis of phloridzin caused stunted growth in *MdUGT88F1* silencing lines, which was verified further by our study and Dare et al. (2017), who used a phloridzin compensation assay.

Dwarf phenotypes in both *CHS* and *UGT88F1* silencing lines were attributed to increased auxin transport, but flavonoids were also changed substantially (Dare et al., 2013; 2017). Flavonoids are regarded by many to be key modulators of auxin transport (Besseau et al., 2007), but there are also reports which seem to contradict this belief (Li et al., 2010; Gallego-Giraldo et al., 2011a). Even so, this does not exclude the possible involvement of auxin in the plant development of *MdUGT88F1* silencing lines. Our data confirmed that phloridzin was a critical compound in modulating the phenylpropanoid pathway flux. Lignin, which is a major structural component of the secondary cell wall, and transgenic plants impaired in lignin biosynthesis frequently exhibit reductions in growth (Li et al., 2010; Gallego-Giraldo et al., 2011a).

In this study, we compared our results carefully with other knockout lines affected in the lignin pathway (Van Acker et al., 2013). Although the decrease in AcBr soluble lignin was comparable with other lignin-reduced plants, the decrease of CWR was very severe. Eventually,

both led to an approximate 35% reduction in total lignin in MdUGT88F1-RNAi lines, which
represented an appreciable reduction. Also, hydroxycinnamoyl derivatives were reduced
significantly in MdUGT88F1-RNAi lines. Decreased levels of of p-coumaryl alcohol and
sinapaldehyde ultimately resulted in large losses of lignin and stunted growth. Moreover,
down-regulations were identified in 9 of the 11 differentially-expressed Laccase (LAC) genes in
MdUGT88F1-RNAi lines (Supplemental Table S2). In addition to peroxidase, laccases are also
necessary for lignin polymerization through the oxidative polymerization of monolignols (Sun et
al., 2018). Consistent with this, down-regulation of UGT88F1 also resulted in large reductions of
hydroxycinnamoyl derivatives and smaller stem xylem region (Dare et al., 2017). In addition, a
metabolome and RNA-seq analysis revealed that increased expression of GolS and decreased
glucose levels were likely responsible for the myo-inositol reduction in MdUGT88F1-RNAi lines
(Valluru and den Ende, 2011). After myo-inositol was depleted, a strong reduction in growth was
observed MdUGT88F1-RNAi lines. Moreover, the myo-inositol reduction was accompanied by
modifications of pectic materials. As a versatile compound, myo-inositol is essential for plant
growth (Cui et al., 2013; Ye et al., 2016) and is involved in the production of cell wall
polysaccharides (Valluru and den Ende, 2011). Thus, the severely dwarfed phenotype among the
MdUGT88F1-RNAi apple lines with decreased phloridzin biosynthesis was related closely to
interference with cell wall deposition (i.e., decreased lignin levels and disorders of cell wall
polysaccharides).
SA was previously shown to cause reduced growth of plants with down-regulated lignin
(Gallego-Giraldo et al., 2011ab). In MdUGT88F1 silencing lines, decreased p-coumaric acid and
stable cinnamic acid levels indicated enhanced metabolic flux into SA biosynthesis (Supplemental
Table S3). Along with increased SA levels, the SA marker genes PRs and the SA biosynthesis
regulatory genes ENHANCED DISEASE SUSCEPTIBILITY 1 (EDS1) and PHYTOALEXIN
DEFICIENT 4 (PAD4) were also induced substantially in MdUGT88F1-RNAi lines
(Supplemental Table S2). Also, the release of pectic elicitors from underlignified secondary cell
walls in lignin-reduced plants induced SA accumulation (Gallego-Giraldo et al., 2011ab).
Consistently, the WS-pectic materials increased at the expense of EDTA-pectins in

key precursor of cell wall polysaccharides. A decrease in myo-inositol was previously shown to

MdUGT88F1-RNAi lines. This modification was verified by decreased myo-inositol, which is a

trigger SA-dependent programmed cell death (PCD) in plants (Chaouch and Noctor, 2010; Bruggeman et al., 2015). Thus, it was likely that increased SA levels were attributed to spillover from the phenylpropanoid pathway and *myo*-inositol-dependent release of pectic elicitors in MdUGT88F1-RNAi apple lines.

Our study also suggested that in MdUGT88F1-RNAi lines, decreased phloridzin biosynthesis enhanced Valsa canker resistance by increasing the SA level through indirect modulation of cell wall deposition. SA signaling predominantly combats biotrophic pathogens and viruses, whereas jasmonic acid (JA) signaling is critical for the response to necrotrophic pathogens and insects (Glazebrook, 2005; Vlot et al., 2009). Generally, V. mali is considered to be a necrotrophic pathogen (Yin et al., 2015). However, Valsa canker resistance would be independent of JA in transgenic apple lines (Supplemental Fig. S9A). The role of SA in plant defense is frequently associated with the accumulation of ROS and the activation of diverse groups of defense-related genes, which mediate a hypersensitive response (HR, a fast PCD) (Apel and Hirt, 2004; Vlot et al., 2009; Daudi et al., 2012). PCD is believed to be detrimental to biotrophic and hemibiotrophic pathogens, because of a reduction of vivosphere and restriction of hyphae extension, but beneficial to infections caused by necrotrophic pathogens (Gilchrist, 1998). Here, we revealed a positive potential of SA in Valsa canker resistance in apple. Similarly, Yin et al. (2016a) found that genes involved in apple SA signaling were significantly up-regulated after V. mali infection. To counteract SA-induced defense responses, V. mali may have acquired a salicylate hydroxylase gene (which encodes an enzyme that degrades SA) through horizontal gene transfer from bacteria (Tanaka et al., 2015; Yin et al., 2016b).

In MdUGT88F1-RNAi lines, there were higher pre-challenge levels of ROS, although little induction of H_2O_2 was identified upon infection with V. mali. Increased ROS levels were attributed mainly to a compromised antioxidant system, which included decreases in phloridzin, hydroxycinnamoyl derivatives, GSSH, GSH, and AsA (Wang et al., 2012). Furthermore, the contrasting H_2O_2 dynamics in susceptible ZD1 and resistant ZH16 line indicated that oxidative burst may be a key factor for Valsa canker resistance in apple. It has been observed previously that H_2O_2 can induced the accumulation of SA, and vice versa (Guo et al., 2017). In susceptible ZD1, the loss of key modulator(s) in the positive feedback loop of SA and ROS made it necessary to investigate further the role of ROS in Valsa canker resistance in apple.

ROS act as antimicrobial molecules and are important signals that mediate plant disease resistance. However, excessive ROS can be phytotoxic (Suzuki et al., 2011). Necrotrophs are defined as pathogens that derive energy from dying or dead plant tissues, but they differ substantially in the progression of pathogenesis, ranging from rapidly killing host cells, such as *Botrytis cinerea*, to having an extended asymptomatic phase before killing host cells, such as *Alternaria alternata* (Oliver et al., 2012; Meng et al., 2018). Recently, it was suggested that suppressing PCD probably played an important role in infections by *V. mali. V. mali* may not need to kill host cells rapidly, but instead may regulates their death to enable successful colonization over time (Zhang et al., 2018). In the present study, we showed that JA does not appear to be involved in *Valsa* canker resistance in apple (Supplemental Fig. S9B, 9C). We speculated that *V. mali* could be a heminecrotrophic or hemibiotrophic pathogen.

421

422

423

424

425

426

427

428

429

430

431

432

433

434

435

436

437

438

439

440

441

442

443

444

445

446

447

448

449

450

We also considered that phloridzin may be utilized directly as a sugar alternative and a toxin accelerator by V. mali in apple. Large quantities of glucose from the internal stock of phloridzin released by the action of β -glucosidase might act as a complementary source of carbohydrates and favor the fast multiplication of V. mali. A similar case was characterized in fire blight (Erwinia amylovora) (Gaucher et al., 2013b). In that case, the aglycone phloretin from phloridzin deglycosylation was degraded rapidly into toxins by V. mali, which facilitated establishment of infection and lesion expansion (Koganezawa and Sakuma, 1982; Natsume et al., 1982; Wang et al., 2014). We also found that phloridzin may facilitate toxin production by V. mali through signalling pathways, rather than acting simply as metabolites for toxin production. Meanwhile, upon infection with V. mali, apple optimized its Valsa canker response through self-regulation. Down-regulations of UGT88F1 and UGT88F4 were identified in both susceptible ZD1 and resistant ZH16 after infection, although both PAL and CHS were induced. We verified that a higher level of phloridzin compromised Valsa canker resistance slightly in MdUGT88F1-OE apple lines following V. mali infection. In contrast, in MdUGT88F1-RNAi apple lines, decreased phloridzin biosynthesis and lower glucose levels limited the growth and infection of V. mali directly. In addition, the tightly organized tissues (e.g., compact epidermis and thickened bark regions) limited V. mali colonization and its spread. In particular, MdUGT88F1-RNAi apple stems were characterized by thickened bark and reduced xylem (Dare et al., 2017). Past work has shown that V. mali mainly infected host bark and resulted in tissue necrosis, but it could not degrade

xylem vessels effectively (Yin et al., 2015). In our investigation, we found that resistant apple trees were characterized primarily by tough bark.

Overall, many pleiotropic changes were induced by *MdUGT88F1* silencing (e.g., increases in SA level and *PR* expression, decreases in lignin and *myo*-inositol content, and changes in cell morphology and tissue). However, it is still unclear how decreased phloridzin biosynthesis resulted directly in these pleiotropic changes in MdUGT88F1-RNAi apple lines. Moreover, these changes enhanced resistance to *Valsa* canker along with the direct role played by phloridzin as a sugar alternative and a toxin accelerator by *V. mali* through a cocktail effect. However, the extent to which these changes contributed to pathogen susceptibility remains unclear; this needs to be investigated in the future. Anyhow, we still believe it is promising to coordinate apple growth vigor and pathogen resistance by regulating biosynthesis of MdUGT88F1-mediated phloridzin accurately.

CONCLUSIONS

In conclusion, we proposed a putative working model for phloridzin biosynthesis which is necessary for regulating plant development and *Valsa* canker resistance in apple (Fig. 10). In nature, a normal level of phloridzin biosynthesis maintains well-balanced cell wall deposition and supports vigorous growth in apple. However, following infection with *V. mali*, MdUGT88F1-mediated phloridzin biosynthesis is decreased through a presently unknown mechanism. This causes lignin reduction and disorders of cell wall polysaccharides by indirectly modulating flux through the phenylpropanoid pathway and *myo*-inositol metabolism, respectively. Modified cell wall deposition subsequently stimulates accumulation of SA and ROS. Although modified cell wall deposition results in growth reductions, tissue reinforcements (e.g., in epidermis and bark) ultimately inhibit infection by *V. mali* along with increases in SA and ROS. Meanwhile, decreased phloridzin biosynthesis delays growth and toxin production of *V. mali*, and promotes ROS accumulation, ultimately optimizing apple trees for defense against *V. mali*.

MATERIALS AND METHODS

Materials and growth conditions

Seeds of Arabidopsis thaliana 'Col-0' and homozygous T3 transgenic lines were

surface-sterilized and plated on Murashige and Skoog (MS) medium. After stratification at 4°C for 3 d, the plates were exposed to white light (PAR of 100 to 150 μE m⁻² s⁻¹) for 10 d. The light-grown seedlings were transferred to soil and grown at 22°C under a 16 h light/8 h dark cycle.

The mature leaves of 'Royal Gala' were used in gene and promoter cloning. GL-3, which is a line with a high regeneration capacity isolated from 'Royal Gala', was used in genetic transformation (Dai et al., 2013). GL-3 tissue-cultured plants were subcultured every 4 weeks. After rooting on MS agar medium, transgenic and non-transgenic apple (*Malus domestica*) plantlets were transferred to small plastic pots (8 × 8 cm) that contained a mixture of soil/perlite (1: 1, v:v). After 15 d of acclimation in a growth chamber, the plants were moved to large plastic pots filled with soil and grown in the glasshouse. They were watered regularly and supplied with half-strength Hoagland's nutrient solution (pH 6.0) once a week.

One-year-old twigs of the same size from healthy trees of 68 *Malus* accessions were collected from July to August of 2017 (Supplemental Table S4) from the Horticultural Experimental Station of Northwest A&F University, Yangling (34°20 N, 108°24 E), China, and were subsequently used in the correlation analysis between DHCs and *Valsa* canker resistance. The *Valsa mali* strain 03-8 was cultured on PDA (potato dextrose agar) or PDB (potato dextrose broth) in the dark at 25°C (Yin et al., 2015).

Construction of plasmids and generation of transgenic Arabidopsis and apple plants

To construct transgenic *Arabidopsis* plants that expressed the *GUS* gene driven by the *MdUGT88F1* (*ProMdUGT88F1:GUS*/Col-0) or *MdUGT88F4* (*ProMdUGT88F4:GUS*/Col-0) promoter, 2247-bp and 2230-bp genomic promoter sequences upstream of the coding region of *MdUGT88F1* and *MdUGT88F4* were amplified separately and transferred to the binary vector pGWB433. The resultant constructs were transferred into *Agrobacterium* tumefaciens GV3101, and *Arabidopsis* plants were transformed by the floral dip method (Clough et al., 1998).

To generate transgenic apple lines, the coding region (CDS) of *MdUGT88F1* was cloned and introduced into the vectors pCambia2300 and pGWB411 to create two overexpressing constructs. The vectors pHellsgate2 and pK7WIWG2D were used as RNAi-mediated vectors for silencing *MdUGT88F1*, as described previously (Zhou et al., 2017). Afterwards, *Agrobacterium*-mediated transformation of apple was carried out using GL-3 as the genetic background and strain EHA105

511	(Dai et al., 2013). The primers used for constructing all vectors are shown in Supplemental Table				
512	S5.				
513	RNA extraction, DNA isolation, and RT-qPCR analysis				
514	Total RNA was extracted using a Wolact Plant RNA Isolation Kit (Wolact, Hongkong, China).				
515	Genomic DNA was isolated with a Wolact Plant Genomic DNA purification Kit (Wolact). The				
516	RT-qPCR analysis was carried out as previously described (Zhou et al., 2017). Primers used are				
517	listed in Supplemental Table S5.				
518	Quantification of dihydrochalcones (DHCs)				
519	Quantification of DHCs (including phloretin, phloridzin, trilobatin, and sieboldin) in Malus				
520	samples was performed as described previously (Zhou et al., 2017; 2018).				
521	Morphology Analysis				
522	Shoot height, stem diameter, node number, branch number, leaf length and width, and root				
523	dry weight were measured directly after harvesting. Total root length, root surface area, root				
524	volume, and average diameter and forks were measured using a Winrhizo 2002 (Regent				
525	Corporation, Canada). At least five biological replicates were performed for each measurement.				
526	Complementation and depletion assays				
527	For the complementation assay, the main shoots of GL-3 and transgenic apple plantlets after				
528	4 weeks of subculturing were cut into 1.5-cm segments that included the first two leaves, and then				
529	these cuttings were transplanted in sub-culture MS medium that contained either 0.1% (v/v) ethyl				
530	alcohol or 250 μ M phloridzin dissolved in ethyl alcohol under long-day conditions (14h: 10h, light:				
531	dark cycle) at 23°C. Plants were photographed and growth parameters were recorded after 80 d of				
532	sub-culture. For the depletion assay, the 1.5-cm segments were transplanted either in normal				
533	medium or myo-inositol-depleted MS regeneration medium. After 35 d of treatment, plants were				
534	photographed and growth parameters were measured.				
535	GUS Staining				
536	GUS staining was performed as described by Guo et al. (2017).				
537	Histochemical Analysis				
538	Tissue was excised from stems, leaves, and roots of 38-d-old transgenic apple lines and GL-3				
539	and fixed in an FAA (formalin-aceto-alcohol) solution for 24 h. The fixed tissues were dehydrated				

using a series of different ethanol concentrations, permeated with wax, and embedded in wax. Sections were sliced at a thickness of 10 µm for toluidine blue O and for Mäule and Wiesner staining (Nakashima et al., 2008; Trabucco et al., 2013).

Determination of lignin and cell wall polysaccharide concentrations

The stems and roots of transgenic apple lines and GL-3 were dried at 45°C for 14 d and then milled to a fine powder. The lignin content was determined with CWR (cell wall residue) using the AcBr method (Van Acker et al., 2013). The cellulose content of stems was measured according to Saleme et al. (2017). Extraction and measurement of pectic materials were described by Gallego-Giraldo et al. (2011a).

Assays of infection, fungal growth, and toxins

The *Valsa mali* strain 03-8 was cultured on PDA for 3 d. Agar plugs (5 mm each) were taken from the margin of the growing colony of the strain. One-year-old twigs of the same size from healthy apple trees and both stems (2-month-old) and expanding leaves (38-d-old) of the transgenic apple line and GL-3 were inoculated using stab-inoculation (leaves) and the hole puncher wounding method (twigs and stems) (Wei et al., 2010). Inoculated leaves and stems were incubated at 25°C for 3 d, and inoculated twigs were incubated at 25°C for 6 d. The lesion sizes of leaves were measured by the crossing method. The total length of longitudinal lesions along twigs and stems was measured directly as the size of the lesions. All leaves and bark (15-cm-length twigs) were collected, immediately frozen in liquid nitrogen, and stored at -80°C before analysis of gene expression, dihydrochalcones levels, enzymatic activity, phytohormone content, and H_2O_2 level.

To evaluate the effects of phloridzin and phloretin on growth of strain 03-8, agar plugs (5 mm each) from the margin of one growing colony on PDA were incubated on normal and glucose-depleted PDA/PDB with or without phloridzin or phloretin. Growth rates of strain 03-8 were calculated using the expansion of the colony diameters or OD₆₀₀ values. The residual liquid of the incubated PDB was used to determine DHCs quantitatively after strain 03-8 was removed using centrifugation and a 0.22-μm syringe filter. Meanwhile, the toxic effects of the residual liquid from the PDB culture of *V. mali* on leaves of 2-month-old *M. prunifolia* (obtained from tissue-culture) grown in a greenhouse were measured by the simple leaf-puncture assay. A 20-μL aliquot was inoculated in punctured leaves once a day for five successive days.

Assays for enzymatic activity

The activity of β -Glucosidases (EC 3.2.1.21, β -Glu) of apple bark in response to infection of *Valsa mali* was measured as described by Gaucher et al. (2013b).

Measurement of phytohormone levels

SA and JA were extracted and purified as described in Fu et al. (2012). Briefly, a 50-μL aliquot of extracting solution was air-dried with nitrogen gas before being dissolved in 250 μL sodium acetate (0.1 M, pH 5.5), after which it was treated with 10 μL of β-glucosidase (1 U/μL) and hydrolyzed at 37°C for 2 h. After the hydrolysate was denatured in boiling water for 5 min and centrifuged at 13,000 g for 10 min at 4°C to pellet the protein, the supernatant was used to determine total SA content. A 5-μL aliquot was loaded into the LC-MC system (SCIEX, QTRAP5500) equipped with an InertSustain AQ-C18 column (5.0 μm particle size, 4.6 mm×150 mm; GL Sciences Inc., Tokyo, Japan) at a flow rate of 0.7 mL/min. The solvent system consisted of water that contained 0.1% (v/v) formic acid (A) and methanol (B). The gradient followed 75% A (0 min), 75% A (1 min), 5% A (5 min), 5% A (6.5 min), 75% A (6.6 min), and 75% A (13 min).

Evaluation of H₂O₂ and O₂

Accumulations of H_2O_2 and O_2 were examined by histochemical staining methods that used DAB and NBT, respectively (Hu et al., 2018). Quantitative H_2O_2 measurement was performed using detection kits based on the manufacturer's instructions (Suzhou Comin Biotechnology Co., Ltd, Suzhou, China).

Metabolome analysis

The fourth and fifth leaves of 38-day-old GL-3 and RNAi apple lines from the top of each plant were collected, frozen immediately in liquid nitrogen, and stored at -80 °C. Then, the leaves were delivered to Metware Biotechnology Co., Ltd. (Wuhan, China) to analyze the widely targeted metabolome (Chen et al., 2013). Soluble sugars and sugar alcohols were verified according to the protocol of Hu et al. (2018).

RNA-Sequencing

The plant materials used for RNA-seq analysis were the same as the materials used in the metabolome analysis. After filtrating the adapter and low-quality reads, clean reads were aligned to the reference genome GDDH13 of apple (https://iris.angers.inra.fr/gddh13/the-apple-genome-downloads.html) by HISAT2 (Kim et al.,

2015). FeatureCounts (Liao et al., 2014) was used to count the reads numbers that were mapped to
each gene. DESeq2 was applied for differential gene expression analysis (Love et al., 2014). The
resulting P-values were adjusted by the Benjamini-Hochberg' approach to control for a false
discovery rate (FDR). Genes with $ log2Fold\ Change \ge 1$ and FDR < 0.05 were considered to be
expressed differentially. The differentially expressed genes were further analyzed with Gene
Ontology (GO) and KEGG (KEGG: http://www.genome.jp/kegg/) analysis. ClusterProfiler
software was adopted for GO enrichment analysis (Yu et al., 2012), and the Benjamini and
Hochberg' approach was also used to test the statistical enrichment of differentially expressed
genes in the KEGG pathway.

Statistical Analysis

SPSS software (version 17.0) was used for statistical analysis. Data were subjected to one-way ANOVA and reported as the mean \pm standard deviation (SD).

Accession Numbers

Sequence data from this paper can be found in the GenBank/EMBL data libraries under the following accession numbers: MdUGT88F1(KX639791), MdUGT88F4 (KX639792), MdPh-4'-OGT (AY786997), MdPAL (XM 008389362.2), MdCHS (AAY45748), MdCHI (XM 008371941.2), MdPR1 (GU317941), MdPR2 (AY548364.1), MdPR4 (JQ342967.1), MdPR5 (DQ318213.1), MdPR8 (DQ318214.1), MdCOI1 (XM 008383757.2), MdPLD (XM 008375733.2), MdJMT (XM 008389809.2), and VmG6PDH (KC248180).

ACKNOWLEDGMENTS

This study was sponsored by National Key Research and Development Program of China (2018YFD1000300) and by the Earmarked Fund for China Agriculture Research System (CARS-27). The authors are grateful to Dr. Zhihong Zhang for providing tissue-cultured GL-3 plants and to Prof. Lili Huang for providing *Valsa mali* strain 03-8, and to Thomas A. Gavin, Professor Emeritus, Cornell University, for help with editing this paper.

SUPPLEMENTAL DATA

The following supplemental materials are available.

630	Supplemental Figure S1. Identification of transgenic apple lines.
631	Supplemental Figure S2. Phenotypes of the 3-month-old GL-3 and Ri-3.
632	Supplemental Figure S3. Spatial expressions of MdUGT88F1 and MdUGT88F4.
633	Supplemental Figure S4. Cell wall deposition of the stems in the 38-day-old transgenic apple
634	lines and GL-3.
635	Supplemental Figure S5. Relationship between Valsa canker resistance and dihydrochalcones
636	(DHCs) concentration.
637	Supplemental Figure S6. Effects of phloridzin and phloretin on Valsa mali.
638	Supplemental Figure S7. Expression changes in phloridzin biosynthesis-related genes in
639	susceptible ZD1 and resistant ZH16 apple bark in response to Valsa mali infection.
640	Supplemental Figure S8. Involvement of SA (salicylic acid) in Valsa canker resistance in apple.
641	Supplemental Figure S9. Involvement of JA (jasmonic acid) in Valsa canker resistance in apple.
642	Supplemental Table S1. Phenotypes of transgenic and non-transgenic apple plants.
643	Supplemental Table S2. Differentially-expressed genes involved in phloridzin biosynthesis,
644	lignin biosynthesis, myo-inositol metabolism, and plant-pathogen interactions, which were
645	revealed in RNAi apple lines compared with GL-3 by RNA-seq analysis.
646	Supplemental Table S3. Metabolites involved in growth and defense in leaves from RNAi apple
647	lines and GL-3.
648	Supplemental Table S4. DHC profiles and Valsa canker resistance in Malus.
649	Supplemental Table S5. Primers used in this study.
650	
651	
652	
653	
654	
655	
656	
657	
658	
659	

Table 1. DHC profiles of transgenic apple lines and GL-3 (μg g⁻¹ FW, fresh weight). Data are means \pm SD (n = 3, three biological replicates). *** indicates P < 0.001; ** < 0.01. 'nd', not determined.

Tissues	DHCs	GL-3	OE2-7	OE3-4	Ri-3	Ri-6
	Phloridzin	14731.75 ± 488.89	14902.97± 314.81	14753.02 ± 620.25	8029.11 ± 643.45 ***	6125.08 ± 341.55 ***
Leaf	Trilobatin	nd	nd	nd	152.81 ± 10.26	125.75 ± 9.69
	Phloretin	107.42 ±43.58	$123.09\ \pm 29.56$	129.74 ± 30.6	145.73 ± 29.96	83.28 ± 10.33
	Phloridzin	8308.29 ± 333.41	8213.76 ± 391.2	8071.4 ± 379.38	4704.85 ± 386.23 ***	5052.73 ± 722.73 **
Stem	Trilobatin	nd	nd	nd	100.17 ± 9.29	143.24 ± 14.79
	Phloretin	nd	nd	nd	nd	nd
Root	Phloridzin	6475.3 ± 355.73	6565.33 ± 1284.84	6497.38 ± 403.82	2117.73 ± 309.18 ***	2280.12 ± 277.35 ***
	Trilobatin	nd	nd	nd	68.91 ± 15.8	79.98 ± 10.89
	Phloretin	nd	nd	nd	nd	nd

679	FIGURE LEGENDS
680	Figure 1. Biosynthetic pathways of salicylic acid, lignin, and phloridzin. PAL, phenylalanine
681	ammonia lyase; C4H, cinnamate 4-hydroxylase; 4CL, 4-coumarate:CoA ligase; CHS, chalcone
682	synthase; CHI, chalcone isomerase; DH, dehydrogenase; P2'GT, UDP-glucose:phloretin
683	2'-O-glucosyltransferase; P4'GT, UDP-glucose:phloretin 4'-O-glucosyltransferase; ICS,
684	isochorismate synthase; IPL, isochorismate pyruvate lyase; BA2H, benzoic acid-2-hydroxylase;
685	SA, salicylic acid; SAGT, SA glucosyltransferase; HCT, hydroxycinnamoyl CoA: shikimate
686	hydroxycinnamoyl transferase; CCR, cinnamoyl-CoA reductase; C3H, C3-hydroxylase; CSE,
687	caffeoyl shikimate esterase; COMT, caffeic acid O-methyltransferase; F5H, ferulate 5-hydroxylase
688	ALDH, aldehyde dehydrogenase; CoAOMT, caffeoyl-CoA O-methyltransferase; CAD, cinnamyl
689	alcohol dehydrogenase.
690	
691	Figure 2. Decreased phloridzin biosynthesis resulted in severe reductions in growth in apple.
692	(A, B) Phenotypes of 38-day-old transgenic apple lines and GL-3. (C, D) Assay of phloridzin
693	compensation. Data are means \pm SD ($n = 5$, five biological replicates). Values not represented by
694	the same letter are significantly different (P \leq 0.05). MS control and PZ application represent
695	normal and phloridzin-applied MS regeneration medium, respectively. PZ, phloridzin.
696	
697	Figure 3. Down-regulation of phloridzin biosynthesis decreased lignin accumulation in apple
698	(A, B) Stem compositions in the 3-month-old GL-3 and Ri-3. (C) CWR (cell wall residue) content
699	and (D) AcBr (acetyl bromide) total lignin concentration in the stems and roots of GL-3 and Ri-3.
700	Bark was marked with red lines. Data are means \pm SD ($n = 5$ for B, five plants were used for each
701	line; $n = 5$ for C, five biological replicates; $n = 10$ for D, ten biological replicates). In comparison
702	with GL-3, *** indicates $P < 0.001$; ** < 0.01; * < 0.05. "+" and "-" indicate significant increases
703	and decreases, respectively $(P < 0.05)$.

Figure 4. Histochemical and morphological analysis of transgenic apple lines. Toluidine blue O staining of cross-sections of a (A) leaf, (B) stem, and (D) root of GL-3 and transgenic apple lines. (C) Higher magnification of a portion of the stem highlighting the epidermal cells. (E, F) Angles between main and lateral veins of the leaves of GL-3 and Ri-6. (G) Wieser and (H) Mäule

709	staining of the stem cross-sections of GL-3 and transgenic apple lines. Scale bars = 100 μm (A, B,
710	G, and H) or 50 μ m (D). Data are means \pm SD (n = 11, eleven leaves from eleven plants were used
711	for each line). *** indicates significant difference from GL-3 at $P < 0.001$. pl, palisade cells; s,
712	spongy mesophyll; ue, upper epidermis; le, lower epidermis; p, parenchyma; ph, phloem; x, xylem.
713	v, vessel.
714	
715	Figure 5. Decreased phloridzin biosynthesis resulted in disorders in <i>myo</i> -inositol metabolism
716	and cell wall polysaccharides. Levels of (A) glucose and (B) myo-inositol in the leaves of the
717	38-day-old transgenic apple lines and GL-3. (C, D) Assay results of myo-inositol depletions. (E)
718	Compositions of pectic materials in stems of the 38-d-old transgenic apple lines and GL-3. Data
719	are means \pm SD ($n = 3$ for A, B, E, three biological replicates; $n \ge 7$ for D, at least seven biological
720	replicates). In comparison with GL-3, *** indicates $P < 0.001$; ** < 0.01; * < 0.05. Values not
721	represented by the same letter are significantly different (P < 0.05). "+" and "-" indicate
722	significant increases and decreases, respectively (P \leq 0.05). MS control and MI depletion
723	represent normal and myo-inositol-depleted MS regeneration medium, respectively; WS, EDTA,
724	and HCl represent crude cold water, EDTA, and HCl soluble fractions, respectively.
725	
726	Figure 6. Down-regulation of MdUGT88F1 resulted in enhanced resistance to Valsa mali
727	infection. Evaluation results of Valsa canker resistance in the transgenic apple lines and GL-3 by
728	(A, C) leaf and (B, D) stem inoculation. Changes of (E) MdUGT88F1 and (F) MdUGT88F4
729	expressions and (G-I) DHC levels in the leaves of transgenic apple lines and GL-3 in response to V.
730	mali infection. Data are means \pm SD ($n \ge 15$ for C, D, at least fifteen plants (one leaf or stem from
731	each plant) were used for each line; $n = 3$ for E-I, three biological replicates). In comparison with
732	GL-3, *** indicates $P < 0.001$; ** < 0.01; * < 0.05. Values not represented by the same letter are
733	significantly different (P $<$ 0.05). 'nd', not determined; Control, PDA control; Treatment, $V.$ mali
734	infected leaves.
735	
736	Figure 7. Phloridzin directly promotes growth and toxin production of Valsa mali. (A) Effects
737	of phloridzin on V. mali growth after 48-hour culture. Change in (B) phloridzin and (C) phloretin

concentration in culture. (D) Assay of toxins from the 48-hour-culture residues. /+Glc, normal

739	PDB; /-Glc, PDB without glucose; /+Glc+PZ, normal PDB with phloridzin added (0.5 mM);
740	/-Glc+PZ, PDB without glucose and with phloridzin added (0.5 mM); Data are means \pm SD ($n = 4$,
741	four biological replicates). Values not represented by the same letter are significantly different (P <
742	0.05).
743	
744	Figure 8. SA is positively implicated in Valsa canker resistance in RNAi lines. Levels of (A)
745	free and (B) total SA in the leaves from 38-day-old transgenic apple lines and GL-3. (C) Free SA
746	levels of susceptible ZD1 and resistant ZH16 apple bark on day 4 after their infection by V. mali.
747	(D) Expression changes in MdPR genes in the leaves of transgenic apple lines and GL-3 in
748	response to V . mali infection. Data show means \pm SD ($n = 3$, three biological replicates). In
749	comparison with GL-3 or Control, *** indicates $P < 0.001$; ** < 0.01. Values not represented by
750	the same letter are significantly different (P < 0.05). Control, PDA control; Treatment, V. mali
751	infected (C) bark or (D) leaves.
752	
753	Figure 9. Increased ROS accumulation contributed to enhanced Valsa canker resistance in
754	RNAi lines. (A) NBT- and DAB-staining of the leaves of transgenic apple lines and GL-3. (B)
755	Changes in concentration of H ₂ O ₂ in the leaves from transgenic apple lines and GL-3 in response
756	to V. mali infection. Changes in concentration of H ₂ O ₂ in (C) susceptible apple ZD1 and (D)
757	resistant apple ZH16 in response to V . $mali$ infection. Data show means \pm SD ($n = 3$, three
758	biological replicates). Values not represented by the same letter are significantly different (P <
759	0.05). Control, PDA control; Treatment, V. mali infected (B) leaves or (C, D) bark.
760	
761	Figure 10. A model for MdUGT88F1-mediated phloridzin biosynthesis regulating plant
762	development and Valsa canker resistance in apple. In nature, normal phloridzin biosynthesis
763	maintains well-balanced cell wall deposition and supports vigorous growth in apple. After
764	infection by Valsa mali, MdUGT88F1-mediated phloridzin biosynthesis is decreased through an
765	unknown mechanism, which causes lignin reduction and SA accumulation by indirectly changing
766	phenylpropanoid pathway flux. In addition, decreased phloridzin biosynthesis gives rise to
767	disorders of cell wall polysaccharides by indirectly changing myo-inositol metabolism, which also
768	stimulates accumulation of SA. Modified cell wall deposition results in growth reduction, but also

reinforcement of tissue. The reinforced tissue inhibits infection by *V. mali* along with increases in SA and ROS. Also, decreased phloridzin biosynthesis directly delays growth and toxin production of *V. mali* and promotes accumulation of ROS. Eventually, apple trees adjust to *V. mali* infection. Solid and dashed lines refer to direct and indirect effects, respectively.

- 773 Literature Cited
- 774 Abe K., Kotoda N., Kato H., Soejima J. (2007) Resistance sources to Valsa canker (Valsa
- 775 ceratosperma) in a germplasm collection of diverse Malus species. Plant Breeding. 126:
- 776 449-453.
- 777 Apel K., Hirt H. (2004) Reactive oxygen species: metabolism, oxidative stress, and signal
- transduction. Annu Rev Plant Biol. **55:** 373-399.
- 779 Besseau S., Hoffmann L., Geoffroy P., Lapierre C., Pollet B., Legrand M. (2007) Flavonoid
- 780 Accumulation in Arabidopsis Repressed in Lignin Synthesis Affects Auxin Transport and
- 781 Plant Growth. Plant Cell. 19: 148-162.
- 782 Bessho H., Tsuchiya S., Soejima J. (1994) Screening methods of apple trees for resistance to
- 783 *Valsa* canker. Euphytica. 77: 15-18.
- 784 Bruggeman Q., Prunier F., Mazubert C., de Bont L., Garmier M., Luqan R., Benhamed M.,
- 785 **Bergounioux C., Raynaud C., Delarue M.** (2015) Involvement of Arabidopsis Hexokinase1
- in Cell Death Mediated by Myo-Inositol Accumulation. Plant Cell. 27: 1801-1814.
- 787 Chaouch S., Noctor G. (2010) Myo-inositol abolishes salicylic acid-dependent cell death and
- 788 pathogen defence responses triggered by peroxisomal hydrogen peroxide. New Phytol. 188:
- 789 711-718.
- 790 Chen Z., Zheng Z., Huang J., Lai Z., Fan B. (2009) Biosynthesis of salicylic acid in plants.
- 791 Plant Signal Behav. **4:** 493-496.
- 792 Chen W., Gong L., Guo Z., Wang W., Zhang H., Liu X., Yu S., Xiong L., Luo J. (2013) A
- Novel Integrated Method for Large-Scale Detection, Identification, and Quantification of
- 794 Widely Targeted Metabolites: Application in the Study of Rice Metabolomics. Mol Plant. 6:
- 795 1769-1780.
- 796 Clough S.J., Bent A.F. (1998) Floral dip: a simplified method for Agrobacterium-mediated
- 797 transformation of *Arabidopsis thaliana*. Plant J. **16:** 735-743.
- 798 Cui M., Liang D., Wu S. Ma F., Lei Y. (2013) Isolation and developmental expression analysis
- of L-myo-inositol-1-phosphate synthase in four Actinidia species. Plant Physiol Biochem. 73:
- 800 351-358.
- Dai H., Li W., Han G., Yang Y., Ma Y., Li H., Zhang Z. (2013) Development of a seedling clone
- with high regeneration capacity and susceptibility to Agrobacterium in apple. Sci Hortic. 164:

803	202-208.

- **Dare A.P., Hellens R.P.** (2013) RNA interference silencing of CHS greatly alters the growth
- pattern of apple ($Malus \times domestica$). Plant Signal Behav. **8:** e25033.
- Dare A.P., Tomes S., Jones M., McGhie T.K., Stevenson D.E., Johnson R.A., Greenwood D.R.,
- Hellens R.P. (2013) Phenotypic changes associated with RNA interference silencing of
- chalcone synthase in apple ($Malus \times domestica$). Plant J. **74:** 298-410.
- Dare A.P., Yauk Y., Tomes S., McGhie T.K., Rebstock R.S., Cooney J.M., Atkinson R.G.
- 810 (2017) Silencing a phloretin-specific glycosyltransferase perturbs both general
- phenylpropanoid biosynthesis and plant development. Plant J. **91:** 237-250.
- 812 Daudi A., Cheng Z., O'Brien J.A., Mammarella N., Khan S., Ausubel F.M., Bolwell G.P.
- 813 (2012) The apoplastic oxidative burst peroxidase in Arabidopsis a major component of
- pattern-triggered immunity. Plant Cell. **24:** 275-287.
- 815 Dugé de Bernonville T., Guyot S., Paulin J.P., Gaucher M., Loufrani L., Henrion D., Derbré
- 816 S., Guilet D., Richomme P., Dat J.F., Brisset M.N. (2010) Dihydrochalcones: Implication
- 817 in resistance to oxidative stress and bioactivities against advanced glycation end-products and
- vasoconstriction. Phytochemistry. 71: 443-452.
- 819 Feng H., Xu M., Zheng X., Zhu T., Gao X., Huang L. (2017) microRNAs and Their Targets in
- Apple (Malus domestica cv. "Fuji") Involved in Response to Infection of Pathogen Valsa
- 821 *mali*. Front Plant Sci. **8:** 2081.
- 822 Fu J., Chu J., Sun X., Wang J., Yan C. (2012) Simple, rapid, and simultaneous assay of multiple
- 823 carboxyl containing phytohormones in wounded tomatoes by UPLC-MS/MS using single
- SPE purification and isotope dilution. Anal Sci. **28:** 1081-1087.
- 825 Gallego-Giraldo L., Jikumaru Y., Kamiya Y., Tang Y., Dixon R.A. (2011a) Selective lignin
- downregulation leads to constitutive defense response expression in alfalfa (*Medicago sativa*
- 827 *L.*). New Phytol. **190**: 627-639.
- 828 Gallego-Giraldo L., Escamilla-Trevino L., Jackson L., Dixon R.A. (2011b) Salicylic acid
- mediates the reduced growth of lignin down-regulated plants. Proc Natl Acad Sci USA. 20:
- 830 20814-20819.
- Gaucher M., Dugé de Bernonville T., Lohou D., Guyot S., Guillemette T., Brisset M.N., Dat
- **3.F.** (2013a) Histolocalization and physico-chemical characterization of dihydrochalcones:

833	Insight into the role of apple major flavonoids. Phytochemistry. 90: 78-89.
834	Gaucher M., Dugé de Bernonville T., Guyot S., Dat J.F., Brisset M.N. (2013b) Same ammo
835	different weapons: enzymatic extracts from two apple genotypes with contrasted
836	susceptibilities to fire blight (Erwinia amylovora) differentially convert phloridzin and
837	phloretin in vitro. Plant Physiol Biochem. 72: 178-189.
838	Gilchrist D. (1998) Programmed cell death in plant disease: the purpose and promise of cellular
839	suicide. Annu Rev Phytopathol. 36: 393-414.
840	Glazebrook J. (2005) Contrasting mechanisms of defense against biotrophic and necrotrophic
841	pathogens. Annu Rev Phytopathol. 43: 205-227.
842	Gosch C., Halbwirth H., Kuhn J., Miosic S., Stich K. (2009) Biosynthesis of phloridzin in apple
843	(Malus domestica Borkh.). Plant Sci. 176: 223-231.
844	Gosch C., Halbwirth H., Schneider B., Hölscher D., Stich K. (2010) Cloning and heterologous
845	expression of glycosyltransferases from Malus × domestica and Pyrus communis, which
846	convert phloretin to phloretin 2'-O-glucoside (phloridzin). Plant Sci. 178: 299-306.
847	Guo P., Li Z., Huang P., Li B., Shuang F., Chu J., Guo H. (2017) A Tripartite Amplification
848	Loop Involving the Transcription Factor WRKY75, Salicylic Acid, and Reactive Oxyger
849	Species Accelerates Leaf Senescence. Plant Cell. 29: 2854-2870.
850	Gutierrez B.L., Zhong G., Brown S.K. (2018) Genetic diversity of dihydrochalcone content in
851	Malus germplasm. Genet Resour Crop Ev. 65: 1485-1502.
852	Hu L., Zhou K., Li Y., Chen X., Liu B., Li C., Gong X., Ma F. (2018) Exogenous myo-inosito
853	alleviates salinity-induced stress in Malus hupehensis Rehd. Plant Physiol Biochem. 133
854	116-126.
855	Huot B., Yao J., Montgomery B.L., He S.Y. (2014) Growth-defense tradeoffs in plants: a
856	balancing act to optimize fitness. Mol Plant. 7: 1267-1287.
857	Hutabarat O.S., Flachowsky H., Regos I., Miosic S., Kaufmann C., Faramarzi S., Alam M.Z
858	Gosch C., Peil A., Richter K., Hanke M.V., Treutter D., Stich K., Halbwirth H. (2016)
859	Transgenic apple plants overexpressing the chalcone 3-hydroxylase gene of Cosmos
860	sulphureus show increased levels of 3-hydroxyphloridzin and reduced susceptibility to apple

Ke X., Huang L., Han Q., Gao X., Kang Z. (2013) Histological and cytological investigations of

scab and fire blight. Planta. 243: 1213-1224.

861

- the infection and colonization of apple bark by Valsa mali var. mali. Australas Plant Path. 42:
- 864 85-93.
- Kim D., Langmead B., Salzberg S.L. (2015) HISAT: A Fast Spliced Aligner with Low Memory
- Requirements. Nat Methods. 12: 357-360.
- 867 Koganezawa H., Sakuma T. (1982) Possible role of breakdown products of phloridzin in
- symptom development by *Valsa ceratosperma*. Ann Phytopathol Soc Japan. **48:** 521-528.
- 869 Lee Y., Chen F., Gallego-Giraldo L., Dixon R.A., Voit E.O. (2011) Integrative analysis of
- 870 transgenic alfalfa (Medicago sativa L.) suggests new metabolic control mechanisms for
- monolignol biosynthesis. Plos Comput Biol. 7: e1002047.
- 872 León J., Shulaev V., Yalpani N., Lawton M.A., Raskin I. (1995) Benzoic acid 2-hydroxylase, a
- 873 soluble oxygenase from tobacco, catalyzes salicylic acid biosynthesis. Proc Natl Acad Sci
- 874 USA. **92:** 10413-10417.
- 875 Li X., Bonawitz N.D., Weng J., Chapple C. (2010) The Growth Reduction Associated with
- Repressed Lignin Biosynthesis in Arabidopsis thaliana Is Independent of Flavonoids. Plant
- 877 Cell. **22:** 1620-1632.
- 878 Liao Y., Smyth G.K., Shi W. (2014) featureCounts: An Efficient General Purpose Program for
- Assigning Sequence Reads to Genomic Features. Bioinformatics. **30:** 923-930.
- 880 Love M.I., Huber W., Anders S. (2014) Moderated Estimation of Fold Change and Dispersion
- for RNA-Seq Data with DESeq2. Genome Biol. 15: 550.
- 882 Meng D., Li C., Park H.J., González J., Wang J., Dandekar A.M., Turgeon B.G., Cheng L.
- 883 (2018) Sorbitol Modulates Resistance to Alternaria alternata by Regulating the Expression
- of an *NLR* Resistance Gene in apple. Plant Cell. **30:** 1562-1581.
- 885 Nakashima J., Chen F., Jackson L., Shadle G., Dixon R.A. (2008) Multi-site genetic
- modification of monolignol biosynthesis in alfalfa (Medicago sativa): effects on lignin
- composition in specific cell types. New Phytol. **179**: 738-750.
- Natsume H., Seto H., Haruo S., Ôtake N. (1982) Studies on apple canker disease. The necrotic
- toxins produced by *Valsa ceratosperma*. Agric Biol Chem. **46:** 2101-2106.
- 890 Oliver R.P., Friesen T.L., Faris J.D., Solomon P.S. (2012) Stagm Pathology to genomics and
- host resistance. Annu Rev Phytopathol. **50:** 23-43.
- 892 Saleme M.L.S., Cesarino I., Vargas L., Kim H., Vanholme R., Goeminne G., Van Acker R.,

893	Fonseca F C A	Pallidis A	. Voorend W	. Junior J N	Padmakshan	D. Van	Doorsselaere

- 894 J., Ralph J., Boerjan W. (2017) Silencing CAFFEOYL SHIKIMATE ESTERASE affects
- lignification and improves saccharification. Plant Physiol. **175**: 1040-1057.
- 896 Shirley B.W., Kubasek W.L., Storz G., Bruggemann E., Koornneef M., Ausubel F.M.,
- **Goodman H.M.** (1995) Analysis of *Arabidopsis* mutants deficient in flavonoid biosynthesis.
- 898 Plant J. **8:** 659-671
- 899 Sun Q., Liu X., Yang J., Liu W., Du Q., Wang H., Fu C., Li W.X. (2018) MicroRNA528 Affects
- 900 Lodging Resistance of Maize by Regulating Lignin Biosynthesis under Nitrogen-Luxury
- 901 Conditions. Mol Plant. 11: 806-814.
- 902 Suzuki N., Miller G., Morales J., Shulaev V., Torres M.A., Mittler R. (2011) Respiratory burst
- oxidases: the engines of ROS signaling. Curr Opin Plant Biol. 14: 691-699.
- 904 Tanaka S., Han X., Kahmann R. (2015) Microbial effectors target multiple steps in the salicylic
- acid production and signaling pathway. Front Plant Sci. 6: 349.
- 906 Trabucco G.M., Matos D.A., Lee S.J., Saathoff A.J., Priest H.D., Mockler T.C., Sarath G.,
- 907 Hazen S.P. (2013) Functional characterization of cinnamyl alcohol dehydrogenase and
- 908 caffeic acid O-methyltransferase in *Brachypodium distachyon*. BMC Biotechnol. **13:** 61.
- 909 Valluru R., den Ende W.V. (2011) Myo-inositol and beyond-Emerging networks under stress.
- 910 Plant Sci. **181**: 387-400.
- 911 Van Acker R., Vanholme R., Storme V., Mortimer J.C., Dupree P., Boerjan W. (2013) Lignin
- 912 biosynthesis perturbations affect secondary cell wall composition and saccharification yield
- 913 in Arabidopsis thaliana. Biotechnol Biofuels. **6:** 46.
- 914 Vanholme R., Morreel K., Ralp, J., Boerjan W. (2008) Lignin engineering. Curr Opin Plant
- 915 Biol. 1: 278-285.
- 916 Vlot A.C., Dempsey D.A., Klessig D.F. (2009) Salicylic Acid, a Multifaceted Hormone to
- 917 Combat Disease. Annu Rev Phytopathol. 47: 177-206.
- 918 Wang C., Li C., Li B., Li G., Dong X., Wang G., Zhang Q. (2014) Toxins Produced by Valsa
- 919 *mali var. mali* and Their Relationship with Pathogenicity. Toxins. **6:** 1139-1154.
- 920 Wang P., Yin L., Liang D., Li C., Ma F., Yue Z. (2012) Delayed senescence of apple leaves by
- 921 exogenous melatonin treatment: toward regulating the ascorbate-glutathione cycle. J Pineal
- 922 Res. **53**: 11-20.

- 923 Wildermuth M.C., Dewdney J., Wu G., Ausubel F.M. (2001) Isochorismate synthase is required
- to synthesize salicylic acid for plant defence. Nature. **414:** 562-565.
- Wei J., Huang L., Gao Z., Ke X., Kang Z. (2010) Laboratory evaluation methods of apple Valsa
- 926 canker disease caused by Valsa ceratosperma sensu Kobayashi. Act Phytopathol Sin. 40:
- 927 14-20.
- 928 Xiao Z., Zhang Y., Chen X., Wang Y., Chen W., Xu Q., Li P., Ma F. (2017) Extraction,
- 929 identification, and antioxidant and anticancer tests of seven dihydrochalcones from Malus
- 930 'Red Splendor' fruit. Food Chem. **231**: 324-331.
- 931 Yahyaa M., Davidovich-Rikanati M.R., Eyal Y., Sheachter A., Marzouk S., Lewinsohn E.,
- 932 Ibdah M. (2016) Identification and characterization of UDP-glucose: Phloretin
- 933 4'-O-glycosyltransferase from *Malus* × *domestica* Borkh. Phytochemistry. **130:** 47-55.
- 934 Ye W.X., Ren W.B., Kong L.Q., Zhang W.J., Wang T. (2016) Transcriptomic Profiling Analysis
- 935 of Arabidopsis thaliana Treated with Exogenous Myo-Inositol. Plos One. 11: e0161949.
- 936 Yin Z., Liu H., Li Z., Ke X., Dou D., Gao X., Song N., Dai Q., Wu Y., Xu J.R., Kang Z.,
- 937 **Huang L.** (2015) Genome sequence of *Valsa* canker pathogens uncovers a potential
- 938 adaptation of colonization of woody bark. New Phytol. **208**: 1202-1216.
- 939 Yin Z., Ke X., Kang Z., Huang L. (2016a) Apple resistance responses against Valsa mali
- revealed by transcriptomics analyses. Physiol Mol Plant Pathol. **93**: 85-92.
- 941 Yin Z., Zhu B., Feng H., Huang L. (2016b) Horizontal gene transfer drives adaptive colonization
- of apple trees by the fungal pathogen *Valsa mali*. Sci Rep. **6:** 33129.
- 943 Yu G., Wang L., Han Y., He Q. (2012) clusterProfiler: An R Package for Comparing Biological
- Themes Among Gene Clusters. OMICS. **16:** 284-287.
- 945 Zhang X.Z., Zhao Y.B., Li C.M., Chen D.M., Wang G.P., Chang R.F., Shu H.R. (2007)
- 946 Potential polyphenol markers of phase change in apple (*Malus domestica*). J Plant Physiol.
- 947 **164:** 574-580.
- 248 Zhang M., Feng H., Zhao Y., Song L., Gao C., Xu X., Huang L. (2018) Valsa mali Pathogenic
- 949 Effector VmPxE1 Contributes to Full Virulence and Interacts With the Host Peroxidase
- 950 MdAPX1 as a Potential Target. Front Microbiol. 9: 821.
- 951 Zhou K., Hu L., Li P., Gong X., Ma F. (2017) Genome-wide identification of
- glycosyltransferases converting phloretin to phloridzin in *Malus* species. Plant Sci. **265**:

953	131-145.
954	Zhou K., Hu L., Liu B., Li Y., Gong X., Ma F. (2018) Identification of apple fruits rich in
955	health-promoting dihydrochalcones by comparative assessment of cultivated and wild
956	accessions. Sci Hortic. 233: 38-46.

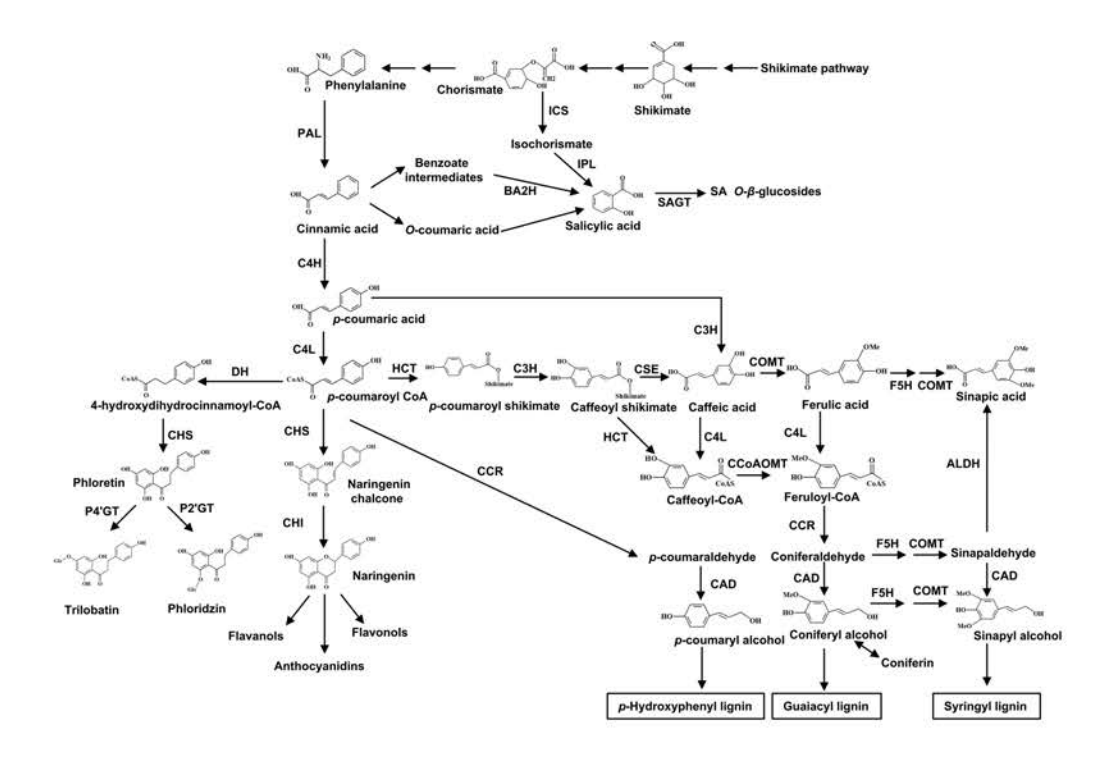


Figure 1. Biosynthetic pathways of salicylic acid, lignin, and phloridzin. PAL, phenylalanine ammonia lyase; C4H, cinnamate 4-hydroxylase; 4CL, 4-coumarate:CoA ligase; CHS, chalcone synthase; CHI, chalcone isomerase; DH, dehydrogenase; P2'GT, UDP-glucose:phloretin 2'-O-glucosyltransferase; P4'GT, UDP-glucose:phloretin 4'-O-glucosyltransferase; ICS, isochorismate synthase; IPL, isochorismate pyruvate lyase; BA2H, benzoic acid-2-hydroxylase; SA, salicylic acid; SAGT, SA glucosyltransferase; HCT, hydroxycinnamoyl CoA: shikimate hydroxycinnamoyl transferase; CCR, cinnamoyl-CoA reductase; C3H, C3-hydroxylase; CSE, caffeoyl shikimate esterase; COMT, caffeic acid O-methyltransferase; F5H, ferulate 5-hydroxylase; ALDH, aldehyde dehydrogenase; CoAOMT, caffeoyl-CoA O-methyltransferase; CAD, cinnamyl alcohol dehydrogenase.

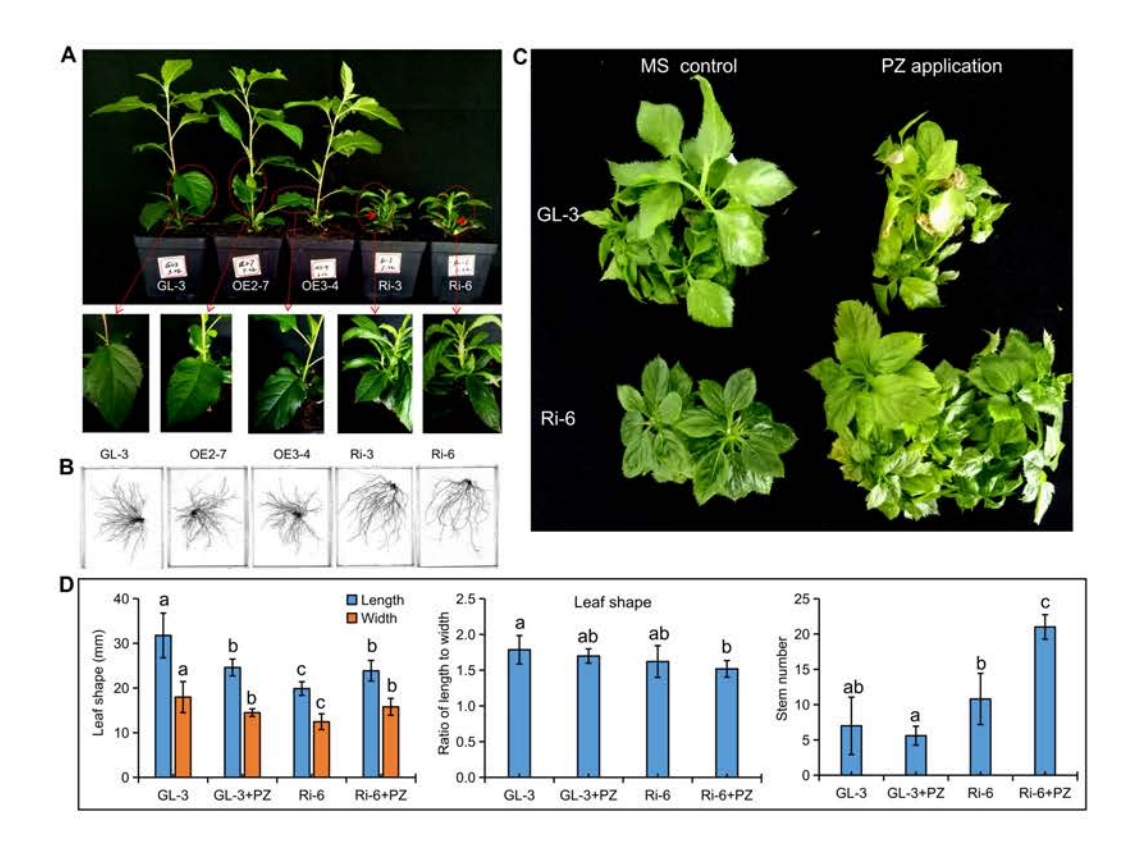


Figure 2. Decreased phloridzin biosynthesis resulted in severe reductions in growth in apple. (A, B) Phenotypes of 38-day-old transgenic apple lines and GL-3. (C, D) Assay of phloridzin compensation. Data are means \pm SD (n = 5, five biological replicates). Values not represented by the same letter are significantly different (P < 0.05). MS control and PZ application represent normal and phloridzin-applied MS regeneration medium, respectively. PZ, phloridzin.

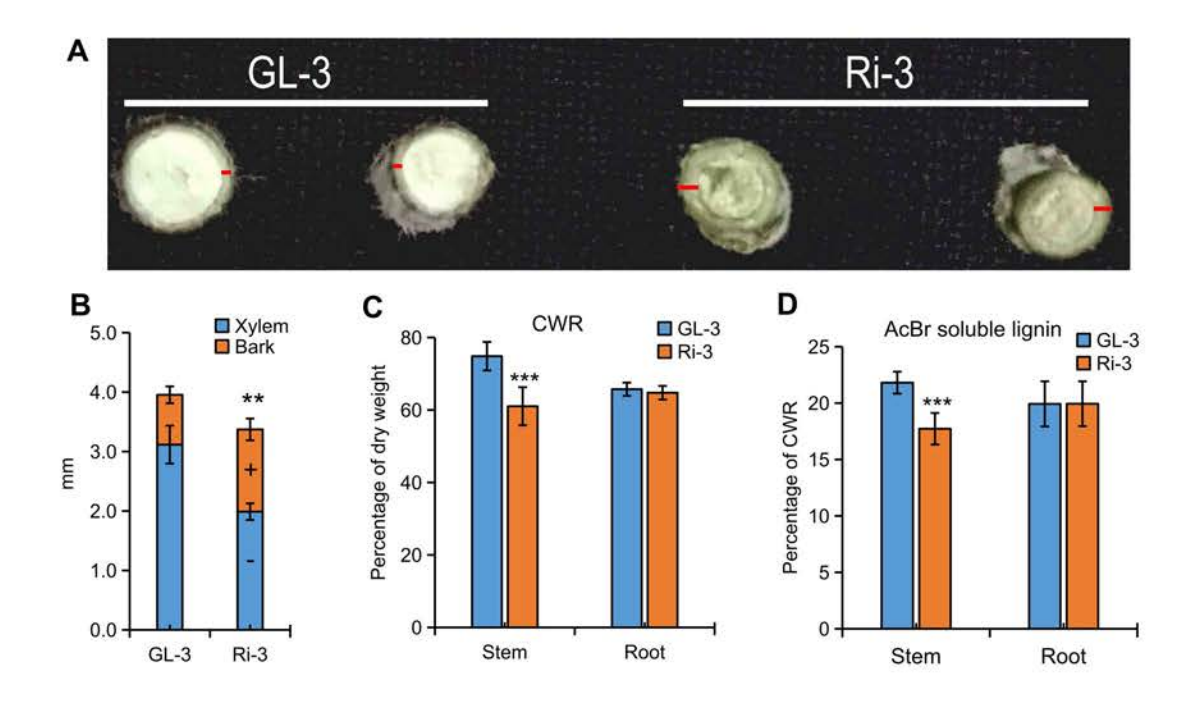


Figure 3. Down-regulation of phloridzin biosynthesis decreased lignin accumulation in apple.

(A, B) Stem compositions in the 3-month-old GL-3 and Ri-3. (C) CWR (cell wall residue) content and (D) AcBr (acetyl bromide) total lignin concentration in the stems and roots of GL-3 and Ri-3. Bark was marked with red lines. Data are means \pm SD (n = 5 for B, five plants were used for each line; n = 5 for C, five biological replicates; n = 10 for D, ten biological replicates). In comparison with GL-3, *** indicates P < 0.001; ** < 0.01; * < 0.05. "+" and "-" indicate significant increases and decreases, respectively (P < 0.05).

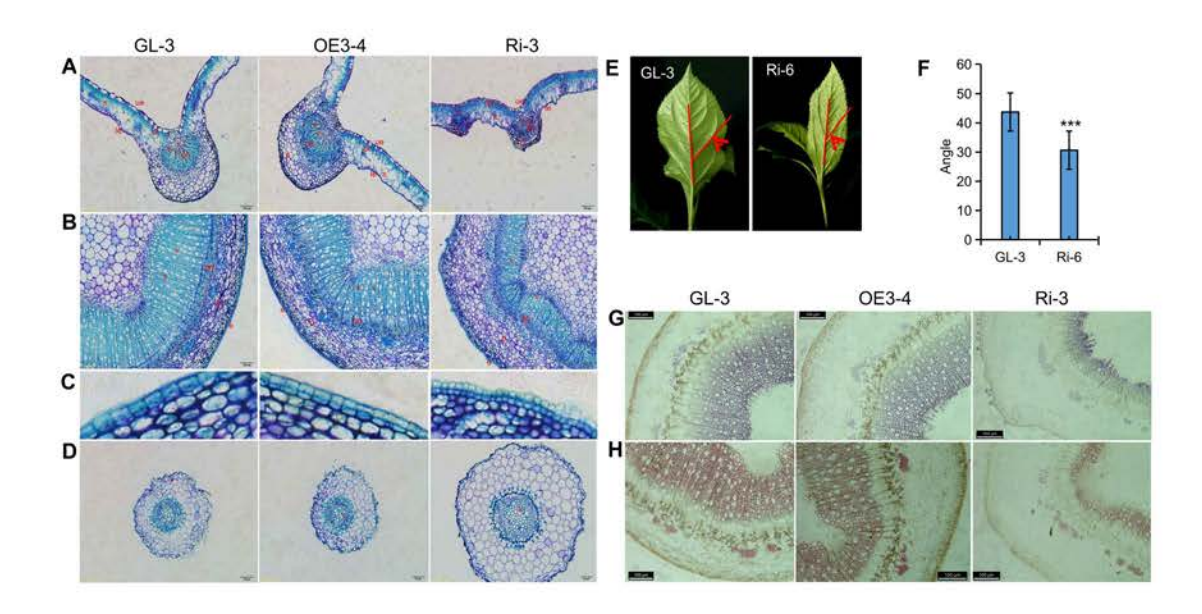


Figure 4. Histochemical and morphological analysis of transgenic apple lines. Toluidine blue O staining of cross-sections of a (A) leaf, (B) stem, and (D) root of GL-3 and transgenic apple lines. (C) Higher magnification of a portion of the stem highlighting the epidermal cells. (E, F) Angles between main and lateral veins of the leaves of GL-3 and Ri-6. (G) Wieser and (H) Mäule staining of the stem cross-sections of GL-3 and transgenic apple lines. Scale bars = $100 \mu m$ (A, B, G, and H) or $50 \mu m$ (D). Data are means \pm SD (n = 11, eleven leaves from eleven plants were used for each line). *** indicates significant difference from GL-3 at P < 0.001. pl, palisade cells; s, spongy mesophyll; ue, upper epidermis; le, lower epidermis; p, parenchyma; ph, phloem; x, xylem. v, vessel.

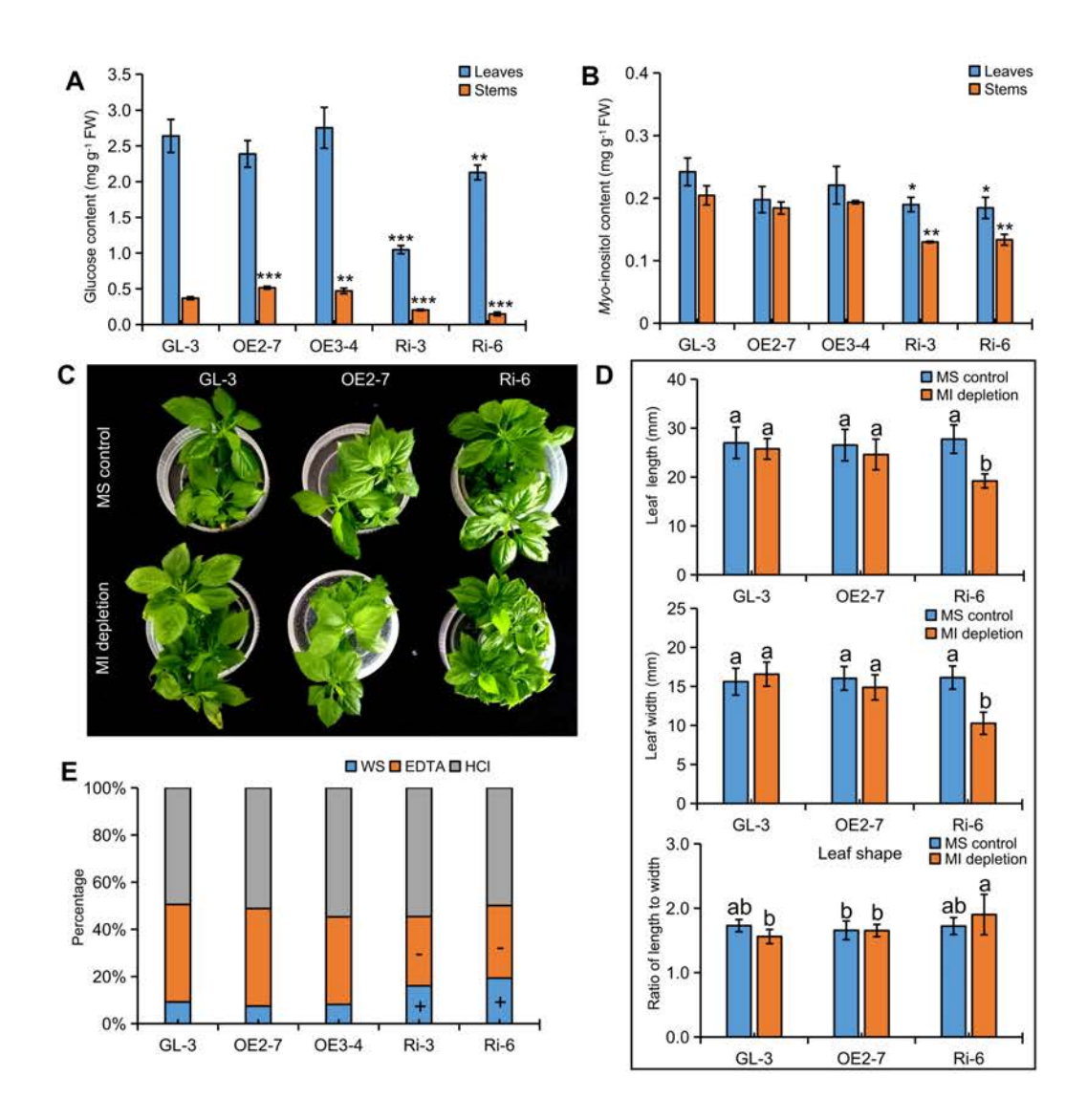


Figure 5. Decreased phloridzin biosynthesis resulted in disorders in *myo*-inositol metabolism and cell wall polysaccharides. Levels of (A) glucose and (B) *myo*-inositol in the leaves of the 38-day-old transgenic apple lines and GL-3. (C, D) Assay results of *myo*-inositol depletions. (E) Compositions of pectic materials in stems of the 38-d-old transgenic apple lines and GL-3. Data are means \pm SD (n = 3 for A, B, E, three biological replicates; $n \ge 7$ for D, at least seven biological replicates). In comparison with GL-3, *** indicates P < 0.001; ** < 0.01; * < 0.05. Values not represented by the same letter are significantly different (P < 0.05). "+" and "-" indicate significant increases and decreases, respectively (P < 0.05). MS control and MI depletion represent normal and *myo*-inositol-depleted MS regeneration medium, respectively; WS, EDTA, and HCl represent crude cold water, EDTA, and HCl soluble fractions, respectively.

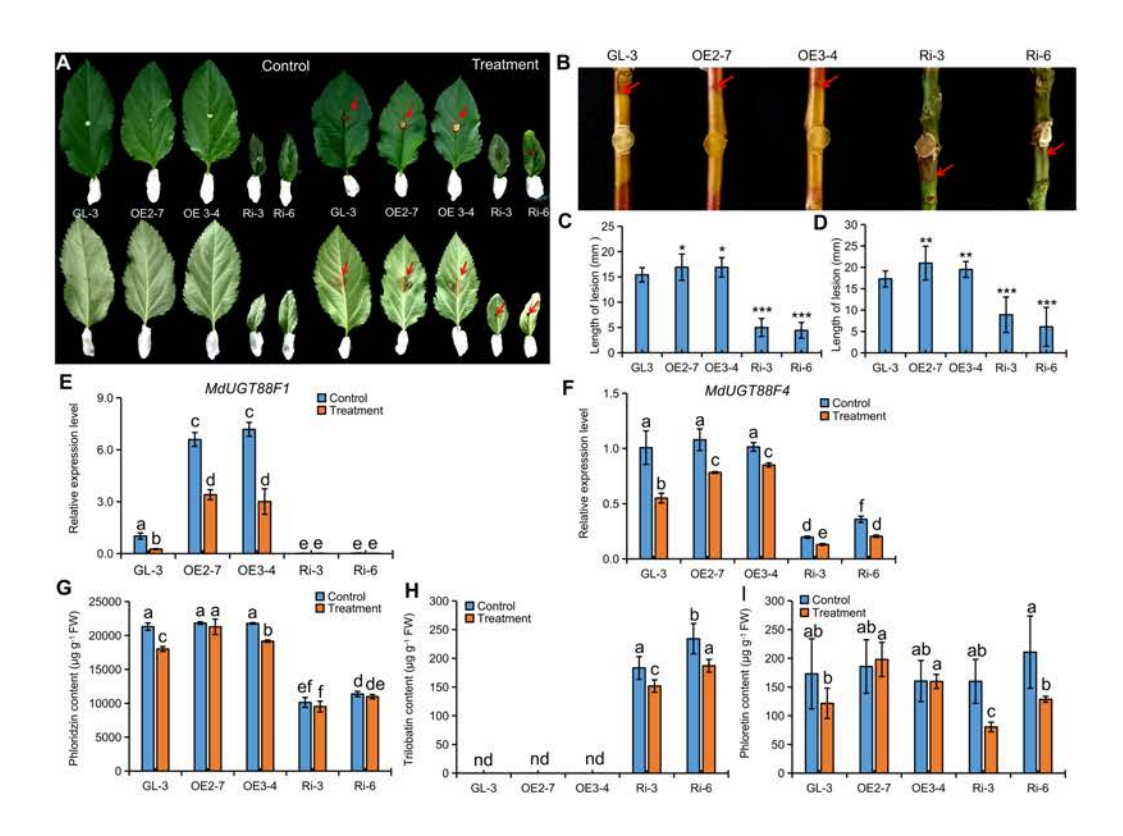


Figure 6. Down-regulation of MdUGT88F1 resulted in enhanced resistance to Valsa mali infection. Evaluation results of Valsa canker resistance in the transgenic apple lines and GL-3 by (A, C) leaf and (B, D) stem inoculation. Changes of (E) MdUGT88F1 and (F) MdUGT88F4 expressions and (G-I) DHC levels in the leaves of transgenic apple lines and GL-3 in response to V. Valsa infection. Data are means Valsa for C, D, at least fifteen plants (one leaf or stem from each plant) were used for each line; Valsa for E-I, three biological replicates). In comparison with GL-3, *** indicates Valsa indicates Valsa for E-I, three biological replicates). In comparison with GL-3, *** indicates Valsa for E-I, three biological replicates). In comparison with GL-3, *** indicates Valsa for E-I, three biological replicates). In comparison with GL-3, *** indicates Valsa for E-I, three biological replicates). In comparison with GL-3, *** indicates Valsa for E-I, three biological replicates). In comparison with GL-3, *** indicates Valsa for E-I, three biological replicates). In comparison with GL-3, *** indicates Valsa for E-I, three biological replicates). In comparison with GL-3, *** indicates Valsa for E-I, three biological replicates). In comparison with GL-3, *** indicates Valsa for E-I, three biological replicates).

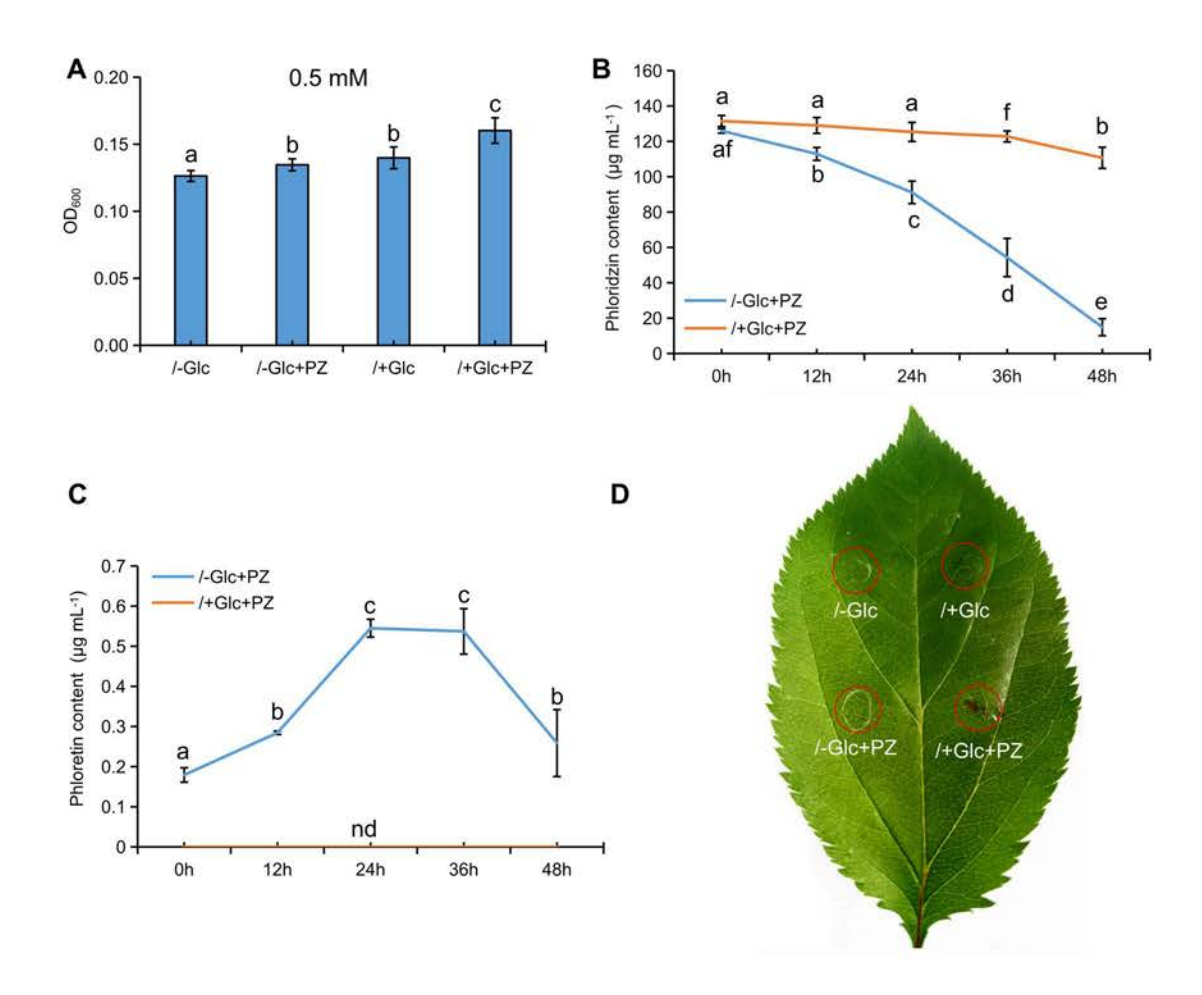


Figure 7. Phloridzin directly promotes growth and toxin production of *Valsa mali*. (A) Effects of phloridzin on *V. mali* growth after 48-hour culture. Change in (B) phloridzin and (C) phloretin concentration in culture. (D) Assay of toxins from the 48-hour-culture residues. /+Glc, normal PDB; /-Glc, PDB without glucose; /+Glc+PZ, normal PDB with phloridzin added (0.5 mM); /-Glc+PZ, PDB without glucose and with phloridzin added (0.5 mM); Data are means \pm SD (n = 4, four biological replicates). Values not represented by the same letter are significantly different (P < 0.05).

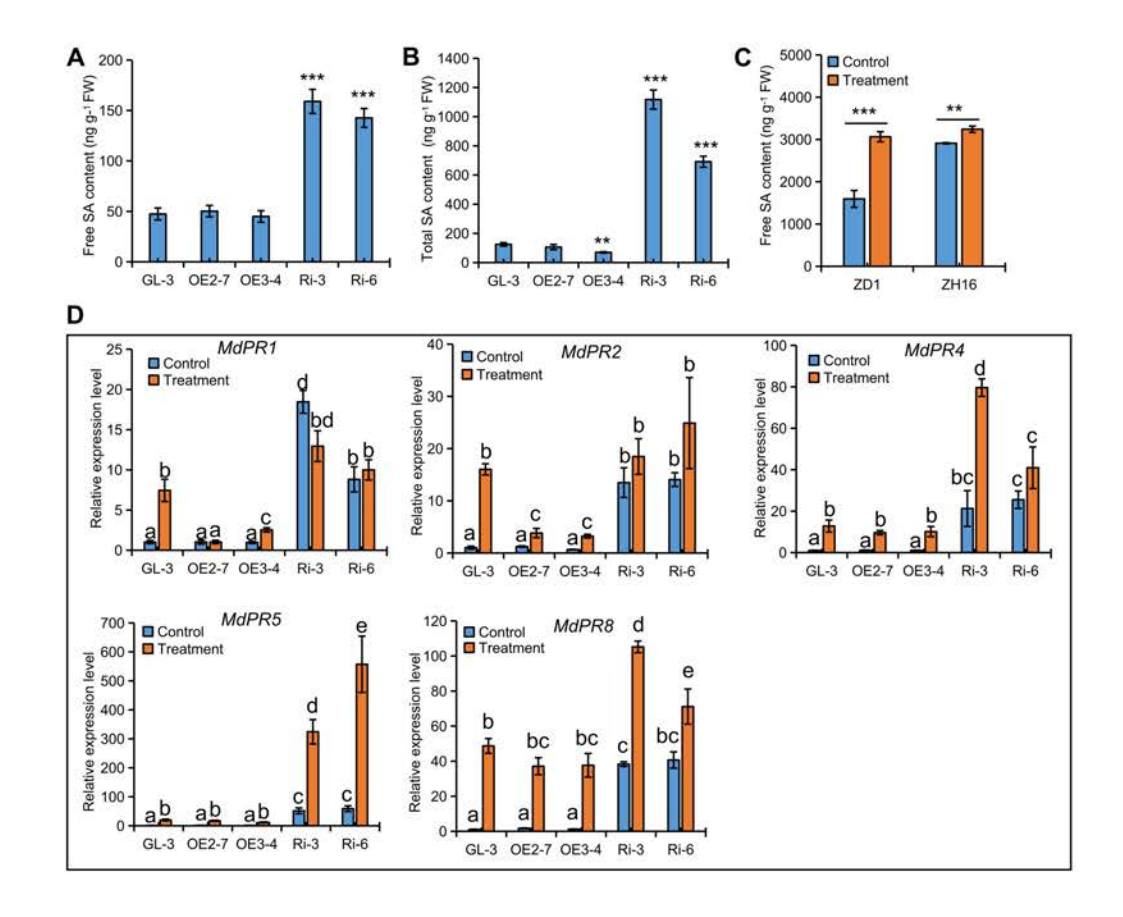


Figure 8. SA is positively implicated in *Valsa* canker resistance in RNAi lines. Levels of (A) free and (B) total SA in the leaves from 38-day-old transgenic apple lines and GL-3. (C) Free SA levels of susceptible ZD1 and resistant ZH16 apple bark on day 4 after their infection by *V. mali*. (D) Expression changes in *MdPR* genes in the leaves of transgenic apple lines and GL-3 in response to *V. mali* infection. Data show means \pm SD (n = 3, three biological replicates). In comparison with GL-3 or Control, *** indicates P < 0.001; ** < 0.01. Values not represented by the same letter are significantly different (P < 0.05). Control, PDA control; Treatment, *V. mali* infected (C) bark or (D) leaves.

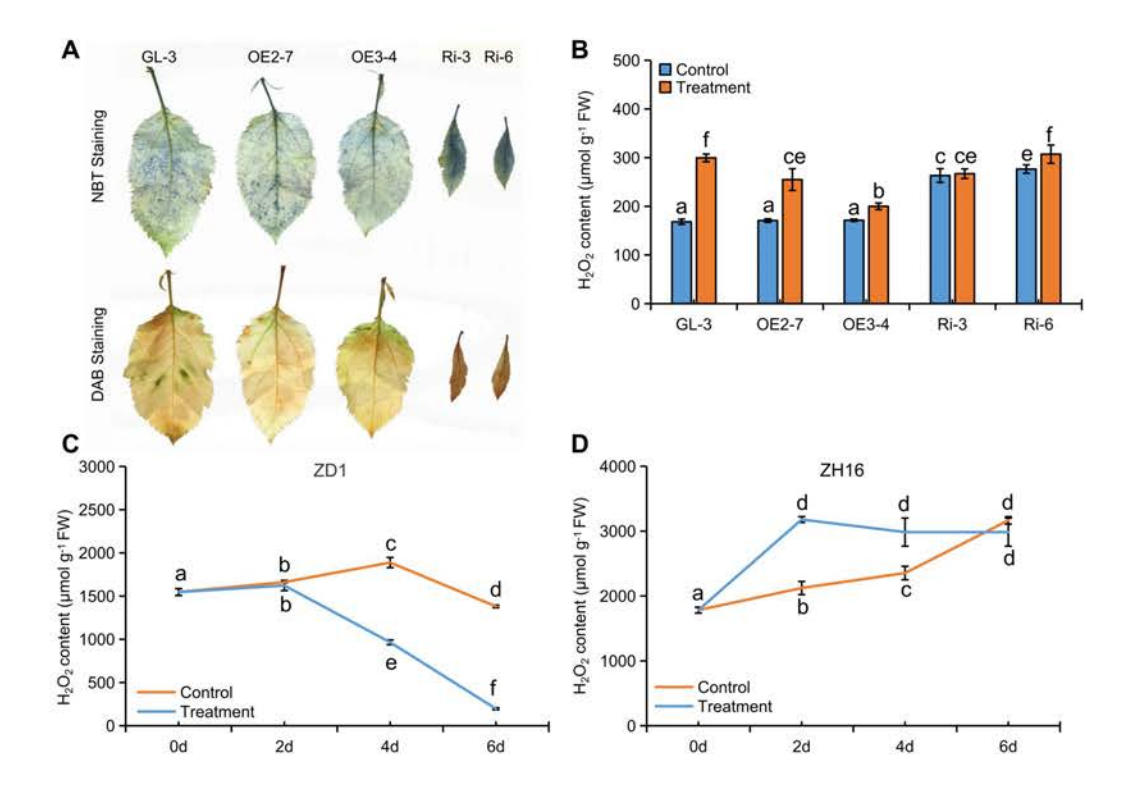


Figure 9. Increased ROS accumulation contributed to enhanced *Valsa* canker resistance in RNAi lines. (A) NBT- and DAB-staining of the leaves of transgenic apple lines and GL-3. (B) Changes in concentration of H_2O_2 in the leaves from transgenic apple lines and GL-3 in response to *V. mali* infection. Changes in concentration of H_2O_2 in (C) susceptible apple ZD1 and (D) resistant apple ZH16 in response to *V. mali* infection. Data show means \pm SD (n = 3, three biological replicates). Values not represented by the same letter are significantly different (P < 0.05). Control, PDA control; Treatment, *V. mali* infected (B) leaves or (C, D) bark.

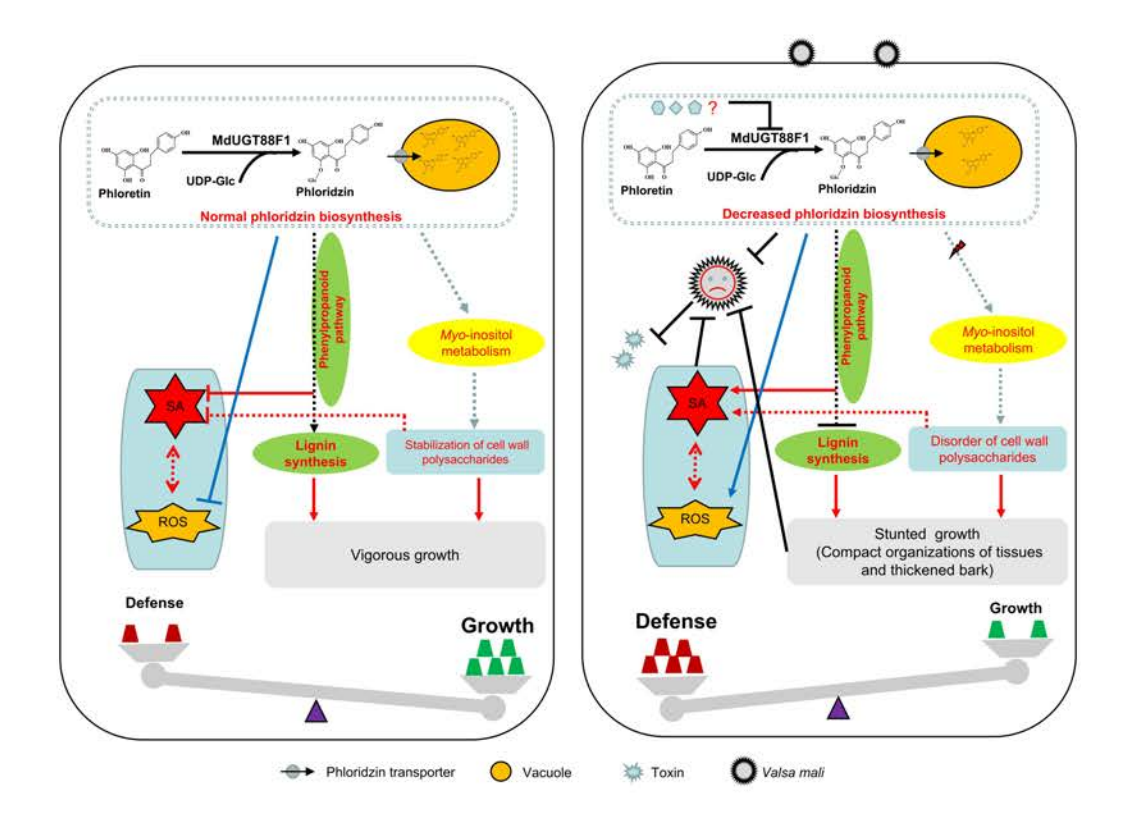


Figure 10. A model for MdUGT88F1-mediated phloridzin biosynthesis regulating plant development and Valsa canker resistance in apple. In nature, normal phloridzin biosynthesis maintains well-balanced cell wall deposition and supports vigorous growth in apple. After infection by Valsa mali, MdUGT88F1-mediated phloridzin biosynthesis is decreased through an unknown mechanism, which causes lignin reduction and SA accumulation by indirectly changing phenylpropanoid pathway flux. In addition, decreased phloridzin biosynthesis gives rise to disorders of cell wall polysaccharides by indirectly changing myo-inositol metabolism, which also stimulates accumulation of SA. Modified cell wall deposition results in growth reduction, but also reinforcement of tissue. The reinforced tissue inhibits infection by V. mali along with increases in SA and ROS. Also, decreased phloridzin biosynthesis directly delays growth and toxin production of V. mali and promotes accumulation of ROS. Eventually, apple trees adjust to V. mali infection. Solid and dashed lines refer to direct and indirect effects, respectively.

Parsed Citations

Abe K., Kotoda N., Kato H., Soejima J. (2007) Resistance sources to Valsa canker (Valsa ceratosperma) in a germplasm collection of diverse Malus species. Plant Breeding. 126: 449-453.

Pubmed: Author and Title

Google Scholar: Author Only Title Only Author and Title

Apel K., Hirt H. (2004) Reactive oxygen species: metabolism, oxidative stress, and signal transduction. Annu Rev Plant Biol. 55: 373-399.

Pubmed: Author and Title

Google Scholar: Author Only Title Only Author and Title

Besseau S., Hoffmann L., Geoffroy P., Lapierre C., Pollet B., Legrand M. (2007) Flavonoid Accumulation in Arabidopsis Repressed in Lignin Synthesis Affects Auxin Transport and Plant Growth. Plant Cell. 19: 148-162.

Pubmed: Author and Title

Google Scholar: Author Only Title Only Author and Title

Bessho H., Tsuchiya S., Soejima J. (1994) Screening methods of apple trees for resistance to Valsa canker. Euphytica. 77: 15-18.

Pubmed: Author and Title

Google Scholar: Author Only Title Only Author and Title

Bruggeman Q., Prunier F., Mazubert C., de Bont L., Garmier M., Luqan R., Benhamed M., Bergounioux C., Raynaud C., Delarue M. (2015) Involvement of Arabidopsis Hexokinase1 in Cell Death Mediated by Myo-Inositol Accumulation. Plant Cell. 27: 1801-1814.

Pubmed: Author and Title

Google Scholar: Author Only Title Only Author and Title

Chaouch S., Noctor G. (2010) Myo-inositol abolishes salicylic acid-dependent cell death and pathogen defence responses triggered by peroxisomal hydrogen peroxide. New Phytol. 188: 711-718.

Pubmed: Author and Title

Google Scholar: Author Only Title Only Author and Title

Chen Z, Zheng Z, Huang J., Lai Z, Fan B. (2009) Biosynthesis of salicylic acid in plants. Plant Signal Behav. 4: 493-496.

Pubmed: Author and Title

Google Scholar: Author Only Title Only Author and Title

Chen W., Gong L., Guo Z, Wang W., Zhang H., Liu X., Yu S., Xiong L., Luo J. (2013) A Novel Integrated Method for Large-Scale Detection, Identification, and Quantification of Widely Targeted Metabolites: Application in the Study of Rice Metabolomics. Mol Plant. 6: 1769-1780.

Pubmed: Author and Title

Google Scholar: Author Only Title Only Author and Title

Clough S.J., Bent AF. (1998) Floral dip: a simplified method for Agrobacterium-mediated transformation of Arabidopsis thaliana. Plant J. 16: 735-743.

Pubmed: Author and Title

Google Scholar: Author Only Title Only Author and Title

Cui M., Liang D., Wu S. Ma F., Lei Y. (2013) Isolation and developmental expression analysis of L-myo-inositol-1-phosphate synthase in four Actinidia species. Plant Physiol Biochem. 73: 351-358.

Pubmed: Author and Title

Google Scholar: Author Only Title Only Author and Title

Dai H., Li W., Han G., Yang Y., Ma Y., Li H., Zhang Z. (2013) Development of a seedling clone with high regeneration capacity and susceptibility to Agrobacterium in apple. Sci Hortic. 164: 202-208.

Pubmed: Author and Title

Google Scholar: Author Only Title Only Author and Title

Dare AP., Hellens R.P. (2013) RNA interference silencing of CHS greatly alters the growth pattern of apple (Malus × domestica). Plant Signal Behav. 8: e25033.

Pubmed: Author and Title

Google Scholar: Author Only Title Only Author and Title

Dare AP., Tomes S., Jones M., McGhie T.K., Stevenson D.E., Johnson R.A, Greenwood D.R., Hellens R.P. (2013) Phenotypic changes associated with RNA interference silencing of chalcone synthase in apple (Malus × domestica). Plant J. 74: 298-410.

Pubmed: Author and Title

Google Scholar: Author Only Title Only Author and Title

Dare A.P., Yauk Y., Tomes S., McGhie T.K., Rebstock R.S., Cooney J.M., Atkinson R.G. (2017) Silencing a phloretin-specific glycosyltransferase perturbs both general phenylpropanoid biosynthesis and plant development. Plant J. 91: 237-250.

Pubmed: Author and Title

Google Scholar: Author Only Title Only Author and Title

Daudi A, Cheng Z, O'Brien J.A, Mammarella N., Khan S., Ausubel F.M., Bolwell G.P. (2012) The apoplastic oxidative burst peroxidase in Arabidopsis a major component of pattern-triggered immunity. Plant Cell. 24: 275-287.

Pubmed: Author and Title

Downloaded from on July 12, 2019 - Published by www.plantphysiol.org
Copyright © 2019 American Society of Plant Biologists. All rights reserved.

Google Scholar: Author Only Title Only Author and Title

Dugé de Bernonville T., Guyot S., Paulin J.P., Gaucher M., Loufrani L., Henrion D., Derbré S., Guilet D., Richomme P., Dat J.F., Brisset M.N. (2010) Dihydrochalcones: Implication in resistance to oxidative stress and bioactivities against advanced glycation end-products and vasoconstriction. Phytochemistry. 71: 443-452.

Pubmed: Author and Title

Google Scholar: Author Only Title Only Author and Title

Feng H., Xu M., Zheng X., Zhu T., Gao X., Huang L. (2017) microRNAs and Their Targets in Apple (Malus domestica cv. "Fuji") Involved in Response to Infection of Pathogen Valsa mali. Front Plant Sci. 8: 2081.

Pubmed: Author and Title

Google Scholar: Author Only Title Only Author and Title

Fu J., Chu J., Sun X., Wang J., Yan C. (2012) Simple, rapid, and simultaneous assay of multiple carboxyl containing phytohormones in wounded tomatoes by UPLC-MS/MS using single SPE purification and isotope dilution. Anal Sci. 28: 1081-1087.

Pubmed: Author and Title

Google Scholar: Author Only Title Only Author and Title

Gallego-Giraldo L., Jikumaru Y., Kamiya Y., Tang Y., Dixon R.A (2011a) Selective lignin downregulation leads to constitutive defense response expression in alfalfa (Medicago sativa L.). New Phytol. 190: 627-639.

Pubmed: Author and Title

Google Scholar: Author Only Title Only Author and Title

Gallego-Giraldo L., Escamilla-Trevino L., Jackson L., Dixon R.A (2011b) Salicylic acid mediates the reduced growth of lignin down-regulated plants. Proc Natl Acad Sci USA 20: 20814-20819.

Pubmed: Author and Title

Google Scholar: Author Only Title Only Author and Title

Gaucher M., Dugé de Bernonville T., Lohou D., Guyot S., Guillemette T., Brisset M.N., Dat J.F. (2013a) Histolocalization and physicochemical characterization of dihydrochalcones: Insight into the role of apple major flavonoids. Phytochemistry. 90: 78-89.

Pubmed: Author and Title

Google Scholar: <u>Author Only Title Only Author and Title</u>

Gaucher M., Dugé de Bernonville T., Guyot S., Dat J.F., Brisset M.N. (2013b) Same ammo, different weapons: enzymatic extracts from two apple genotypes with contrasted susceptibilities to fire blight (Erwinia amylovora) differentially convert phloridzin and phloretin in vitro. Plant Physiol Biochem. 72: 178-189.

Pubmed: Author and Title

Google Scholar: Author Only Title Only Author and Title

Gilchrist D. (1998) Programmed cell death in plant disease: the purpose and promise of cellular suicide. Annu Rev Phytopathol. 36: 393-414.

Pubmed: Author and Title

Google Scholar: Author Only Title Only Author and Title

Glazebrook J. (2005) Contrasting mechanisms of defense against biotrophic and necrotrophic pathogens. Annu Rev Phytopathol. 43: 205-227.

Pubmed: Author and Title

Google Scholar: Author Only Title Only Author and Title

Gosch C., Halbwirth H., Kuhn J., Miosic S., Stich K. (2009) Biosynthesis of phloridzin in apple (Malus domestica Borkh.). Plant Sci. 176: 223-231.

Pubmed: Author and Title

Google Scholar: <u>Author Only Title Only Author and Title</u>

Gosch C., Halbwirth H., Schneider B., Hölscher D., Stich K. (2010) Cloning and heterologous expression of glycosyltransferases from Malus × domestica and Pyrus communis, which convert phloretin to phloretin 2'-O-glucoside (phloridzin). Plant Sci. 178: 299-306.

Pubmed: Author and Title

Google Scholar: Author Only Title Only Author and Title

Guo P., Li Z., Huang P., Li B., Shuang F., Chu J., Guo H. (2017) A Tripartite Amplification Loop Involving the Transcription Factor WRKY75, Salicylic Acid, and Reactive Oxygen Species Accelerates Leaf Senescence. Plant Cell. 29: 2854-2870.

Pubmed: Author and Title

Google Scholar: Author Only Title Only Author and Title

Gutierrez B.L., Zhong G., Brown S.K. (2018) Genetic diversity of dihydrochalcone content in Malus germplasm. Genet Resour Crop Ev. 65: 1485-1502.

Pubmed: Author and Title

Google Scholar: Author Only Title Only Author and Title

Hu L., Zhou K., Li Y., Chen X., Liu B., Li C., Gong X., Ma F. (2018) Exogenous myo-inositol alleviates salinity-induced stress in Malus hupehensis Rehd. Plant Physiol Biochem. 133: 116-126.

Pubmed: Author and Title

Google Scholar: Author Only Title Only Author and Title

Huot B., Yao J., Montgomery B.L., Dev & Mad (2014) Growth-de featse-tPadesifes by plants an halanding act to optimize fitness. Mol Plant. 7:

Copyright © 2019 American Society of Plant Biologists. All rights reserved.

1267-1287.

Pubmed: Author and Title

Google Scholar: Author Only Title Only Author and Title

Hutabarat O.S., Flachowsky H., Regos I., Miosic S., Kaufmann C., Faramarzi S., Alam M.Z., Gosch C., Peil A, Richter K., Hanke M.V., Treutter D., Stich K., Halbwirth H. (2016) Transgenic apple plants overexpressing the chalcone 3-hydroxylase gene of Cosmos sulphureus show increased levels of 3-hydroxyphloridzin and reduced susceptibility to apple scab and fire blight. Planta. 243: 1213-1224.

Pubmed: Author and Title

Google Scholar: Author Only Title Only Author and Title

Ke X., Huang L., Han Q., Gao X., Kang Z. (2013) Histological and cytological investigations of the infection and colonization of apple bark by Valsa mali var. mali. Australas Plant Path. 42: 85-93.

Pubmed: Author and Title

Google Scholar: <u>Author Only Title Only Author and Title</u>

Kim D., Langmead B., Salzberg S.L. (2015) HISAT: A Fast Spliced Aligner with Low Memory Requirements. Nat Methods. 12: 357-360.

Pubmed: Author and Title

Google Scholar: Author Only Title Only Author and Title

Koganezawa H., Sakuma T. (1982) Possible role of breakdown products of phloridzin in symptom development by Valsa ceratosperma. Ann Phytopathol Soc Japan. 48: 521-528.

Pubmed: Author and Title

Google Scholar: Author Only Title Only Author and Title

Lee Y., Chen F., Gallego-Giraldo L., Dixon R.A, Voit E.O. (2011) Integrative analysis of transgenic alfalfa (Medicago sativa L.) suggests new metabolic control mechanisms for monolignol biosynthesis. Plos Comput Biol. 7: e1002047.

Pubmed: Author and Title

Google Scholar: Author Only Title Only Author and Title

León J., Shulaev V., Yalpani N., Lawton M.A, Raskin I. (1995) Benzoic acid 2-hydroxylase, a soluble oxygenase from tobacco, catalyzes salicylic acid biosynthesis. Proc Natl Acad Sci USA 92: 10413-10417.

Pubmed: Author and Title

Google Scholar: Author Only Title Only Author and Title

Li X., Bonawitz N.D., Weng J., Chapple C. (2010) The Growth Reduction Associated with Repressed Lignin Biosynthesis in Arabidopsis thaliana Is Independent of Flavonoids. Plant Cell. 22: 1620-1632.

Pubmed: Author and Title

Google Scholar: Author Only Title Only Author and Title

Liao Y., Smyth G.K., Shi W. (2014) featureCounts: An Efficient General Purpose Program for Assigning Sequence Reads to Genomic Features. Bioinformatics. 30: 923-930.

Pubmed: Author and Title

Google Scholar: Author Only Title Only Author and Title

Love M.I., Huber W., Anders S. (2014) Moderated Estimation of Fold Change and Dispersion for RNA-Seq Data with DESeq2. Genome Biol. 15: 550.

Pubmed: Author and Title

Google Scholar: Author Only Title Only Author and Title

Meng D., Li C., Park H.J., González J., Wang J., Dandekar A.M., Turgeon B.G., Cheng L. (2018) Sorbitol Modulates Resistance to Alternaria alternata by Regulating the Expression of an NLR Resistance Gene in apple. Plant Cell. 30: 1562-1581.

Pubmed: Author and Title

Google Scholar: Author Only Title Only Author and Title

Nakashima J., Chen F., Jackson L., Shadle G., Dixon R.A (2008) Multi-site genetic modification of monolignol biosynthesis in alfalfa (Medicago sativa): effects on lignin composition in specific cell types. New Phytol. 179: 738-750.

Pubmed: Author and Title

Google Scholar: Author Only Title Only Author and Title

Natsume H., Seto H., Haruo S., Ôtake N. (1982) Studies on apple canker disease. The necrotic toxins produced by Valsa ceratosperma. Agric Biol Chem. 46: 2101-2106.

Pubmed: Author and Title

Google Scholar: Author Only Title Only Author and Title

Oliver R.P., Friesen T.L., Faris J.D., Solomon P.S. (2012) Stagm Pathology to genomics and host resistance. Annu Rev Phytopathol. 50: 23-43.

Pubmed: Author and Title

Google Scholar: Author Only Title Only Author and Title

Saleme M.L.S., Cesarino I., Vargas L., Kim H., Vanholme R., Goeminne G., Van Acker R., Fonseca F.C.A, Pallidis A, Voorend W., Junior J.N., Padmakshan D., Van Doorsselaere J., Ralph J., Boerjan W. (2017) Silencing CAFFEOYL SHIKIMATE ESTERASE affects lignification and improves saccharification. Plant Physiol. 175: 1040-1057.

Pubmed: Author and Title

Shirley B.W., Kubasek W.L., Storz G., Bruggemann E., Koornneef M., Ausubel F.M., Goodman H.M. (1995) Analysis of Arabidopsis mutants deficient in flavonoid biosynthesis. Plant J. 8: 659-671

Pubmed: Author and Title

Google Scholar: Author Only Title Only Author and Title

Sun Q., Liu X., Yang J., Liu W., Du Q., Wang H., Fu C., Li W.X. (2018) MicroRNA528 Affects Lodging Resistance of Maize by Regulating Lignin Biosynthesis under Nitrogen-Luxury Conditions. Mol Plant. 11: 806-814.

Pubmed: Author and Title

Google Scholar: Author Only Title Only Author and Title

Suzuki N., Miller G., Morales J., Shulaev V., Torres M.A., Mittler R. (2011) Respiratory burst oxidases: the engines of ROS signaling. Curr Opin Plant Biol. 14: 691-699.

Pubmed: Author and Title

Google Scholar: Author Only Title Only Author and Title

Tanaka S., Han X., Kahmann R. (2015) Microbial effectors target multiple steps in the salicylic acid production and signaling pathway. Front Plant Sci. 6: 349.

Pubmed: Author and Title

Google Scholar: Author Only Title Only Author and Title

Trabucco G.M., Matos D.A, Lee S.J., Saathoff AJ., Priest H.D., Mockler T.C., Sarath G., Hazen S.P. (2013) Functional characterization of cinnamyl alcohol dehydrogenase and caffeic acid O-methyltransferase in Brachypodium distachyon. BMC Biotechnol. 13: 61.

Pubmed: Author and Title

Google Scholar: Author Only Title Only Author and Title

Valluru R., den Ende W.V. (2011) Myo-inositol and beyond-Emerging networks under stress. Plant Sci. 181: 387-400.

Pubmed: Author and Title

Google Scholar: Author Only Title Only Author and Title

Van Acker R., Vanholme R., Storme V., Mortimer J.C., Dupree P., Boerjan W. (2013) Lignin biosynthesis perturbations affect secondary cell wall composition and saccharification yield in Arabidopsis thaliana. Biotechnol Biofuels. 6: 46.

Pubmed: Author and Title

Google Scholar: Author Only Title Only Author and Title

Vanholme R., Morreel K., Ralp, J., Boerjan W. (2008) Lignin engineering. Curr Opin Plant Biol. 1: 278-285.

Pubmed: Author and Title

Google Scholar: Author Only Title Only Author and Title

Vlot A.C., Dempsey D.A, Klessig D.F. (2009) Salicylic Acid, a Multifaceted Hormone to Combat Disease. Annu Rev Phytopathol. 47: 177-206.

Pubmed: Author and Title

Google Scholar: Author Only Title Only Author and Title

Wang C., Li C., Li B., Li G., Dong X., Wang G., Zhang Q. (2014) Toxins Produced by Valsa mali var. mali and Their Relationship with Pathogenicity. Toxins. 6: 1139-1154.

Pubmed: Author and Title

Google Scholar: <u>Author Only Title Only Author and Title</u>

Wang P., Yin L., Liang D., Li C., Ma F., Yue Z. (2012) Delayed senescence of apple leaves by exogenous melatonin treatment: toward regulating the ascorbate-glutathione cycle. J Pineal Res. 53: 11-20.

Pubmed: Author and Title

Google Scholar: <u>Author Only Title Only Author and Title</u>

Wildermuth M.C., Dewdney J., Wu G., Ausubel F.M. (2001) Isochorismate synthase is required to synthesize salicylic acid for plant defence. Nature. 414: 562-565.

Pubmed: Author and Title

Google Scholar: Author Only Title Only Author and Title

Wei J., Huang L., Gao Z, Ke X., Kang Z (2010) Laboratory evaluation methods of apple Valsa canker disease caused by Valsa ceratosperma sensu Kobayashi. Act Phytopathol Sin. 40: 14-20.

Pubmed: Author and Title

Google Scholar: Author Only Title Only Author and Title

Xiao Z, Zhang Y., Chen X., Wang Y., Chen W., Xu Q., Li P., Ma F. (2017) Extraction, identification, and antioxidant and anticancer tests of seven dihydrochalcones from Malus 'Red Splendor' fruit. Food Chem. 231: 324-331.

Pubmed: Author and Title

Google Scholar: Author Only Title Only Author and Title

Yahyaa M., Davidovich-Rikanati M.R., Eyal Y., Sheachter A, Marzouk S., Lewinsohn E., Ibdah M. (2016) Identification and characterization of UDP-glucose: Phloretin 4'-O-glycosyltransferase from Malus × domestica Borkh. Phytochemistry. 130: 47-55.

Pubmed: Author and Title

Google Scholar: <u>Author Only Title Only Author and Title</u>

Ye W.X., Ren W.B., Kong L.Q., Zhang, Mda, Wang, To (2016) Transcriptomin-Brofiling, Analysis of Argbidopsis thaliana Treated with Copyright © 2019 American Society of Plant Biologists. All rights reserved.

Exogenous Myo-Inositol. Plos One. 11: e0161949.

Pubmed: Author and Title

Google Scholar: Author Only Title Only Author and Title

Yin Z, Liu H., Li Z, Ke X., Dou D., Gao X., Song N., Dai Q., Wu Y., Xu J.R., Kang Z, Huang L. (2015) Genome sequence of Valsa canker pathogens uncovers a potential adaptation of colonization of woody bark. New Phytol. 208: 1202-1216.

Pubmed: Author and Title

Google Scholar: <u>Author Only Title Only Author and Title</u>

Yin Z, Ke X., Kang Z, Huang L. (2016a) Apple resistance responses against Valsa mali revealed by transcriptomics analyses. Physiol Mol Plant Pathol. 93: 85-92.

Pubmed: Author and Title

Google Scholar: Author Only Title Only Author and Title

Yin Z, Zhu B., Feng H., Huang L. (2016b) Horizontal gene transfer drives adaptive colonization of apple trees by the fungal pathogen Valsa mali. Sci Rep. 6: 33129.

Pubmed: Author and Title

Google Scholar: Author Only Title Only Author and Title

Yu G., Wang L., Han Y., He Q. (2012) clusterProfiler: An R Package for Comparing Biological Themes Among Gene Clusters. OMICS. 16: 284-287.

Pubmed: Author and Title

Google Scholar: Author Only Title Only Author and Title

Zhang X.Z., Zhao Y.B., Li C.M., Chen D.M., Wang G.P., Chang R.F., Shu H.R. (2007) Potential polyphenol markers of phase change in apple (Malus domestica). J Plant Physiol. 164: 574-580.

Pubmed: Author and Title

Google Scholar: Author Only Title Only Author and Title

Zhang M., Feng H., Zhao Y., Song L., Gao C., Xu X., Huang L. (2018) Valsa mali Pathogenic Effector VmPxE1 Contributes to Full Virulence and Interacts With the Host Peroxidase MdAPX1 as a Potential Target. Front Microbiol. 9: 821.

Pubmed: Author and Title

Google Scholar: Author Only Title Only Author and Title

Zhou K., Hu L., Li P., Gong X., Ma F. (2017) Genome-wide identification of glycosyltransferases converting phloretin to phloridzin in Malus species. Plant Sci. 265: 131-145.

Pubmed: Author and Title

Google Scholar: Author Only Title Only Author and Title

Zhou K., Hu L., Liu B., Li Y., Gong X., Ma F. (2018) Identification of apple fruits rich in health-promoting dihydrochalcones by comparative assessment of cultivated and wild accessions. Sci Hortic. 233: 38-46.

Pubmed: Author and Title

Google Scholar: Author Only Title Only Author and Title